Author's Accepted Manuscript

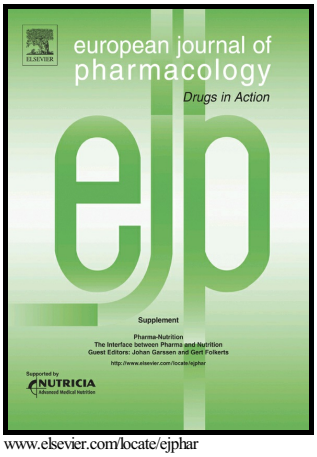

www.elsevier.com/locate/ejphar

Dual effects of the PI3K inhibitor ZSTK474 on multidrug efflux pumps in resistant cancer cells

Divya Muthiah, Richard Callaghan

PII: S0014-2999(17)30576-9
DOI: http://dx.doi.org/10.1016/j.ejphar.2017.09.001
Reference: EJP71387

To appear in: *European Journal of Pharmacology*

Received date: 28 July 2017
Revised date: 30 August 2017
Accepted date: 1 September 2017

Cite this article as: Divya Muthiah and Richard Callaghan, Dual effects of the PI3K inhibitor ZSTK474 on multidrug efflux pumps in resistant cancer cells, *European Journal of Pharmacology,* http://dx.doi.org/10.1016/j.ejphar.2017.09.001

This is a PDF file of an unedited manuscript that has been accepted for publication. As a service to our customers we are providing this early version of the manuscript. The manuscript will undergo copyediting, typesetting, and review of the resulting galley proof before it is published in its final citable form. Please note that during the production process errors may be discovered which could affect the content, and all legal disclaimers that apply to the journal pertain.

ACCEPTED MANUSCRIPT

Dual effects of the PI3K inhibitor ZSTK474 on multidrug efflux pumps in resistant cancer cells

Divya Muthiah & *Richard Callaghan

Division of Biomedical Science & Biochemistry, Research School of Biology and Medical School, The Australian National University, Canberra, Australia

Correspondence:

*Research School of Biology, Building 134, Linnaeus Way, The Australian National University, Acton, Canberra, ACT 2601 Australia

Tel: +61 2 6125 0824

E-mail: richard.callaghan@anu.edu.au

Accepted manuscript

ACCEPTED MANUSCRIPT

Abstract

ZSTK474 is a potent phosphoinositide 3-kinase (PI3K) inhibitor that reduces cell proliferation via G_1-arrest. However, there is little information on the susceptibility of this anticancer drug to resistance conferred by the multidrug pumps P-glycoprotein (ABCB1) and ABCG2. We have demonstrated that ZSTK474 generated cytotoxicity in cells over-expressing either pump with potency similar to that in drug sensitive cells. In addition, the co-administration of ZSTK474 with the cytotoxic anti-cancer drugs vinblastine and mitoxantrone caused a potentiated cytotoxic effect in both drug sensitive and efflux pump expressing cells. These observations suggest that ZSTK474 is unaffected by the presence of multidrug efflux pumps and may circumvent their activities. Indeed, ZSTK474 increased the cellular accumulation of calcein-AM and mitoxantrone in cells expressing ABCB1 and ABCG2, respectively. ZSTK474 treatment also resulted in reduced expression of both efflux pumps in multidrug resistant cancer cells. Measurement of ABCB1 or ABCG2 mRNA levels demonstrated that the reduction was not due to altered transcription. Similarly, inhibitor studies showed that the proteasomal degradation pathway for ABCB1 and the lysosomal route for ABCG2 degradation were unaffected by ZSTK474. Thus the mechanism underlying reduced ABCB1 and ABCG2 levels caused by ZSTK474 was due to a reduction in overall protein synthesis; a process influenced by the PI3K pathway. In summary, ZSTK474 is not susceptible to efflux by the resistance mediators ABCB1 and ABCG2. Moreover, it inhibits the drug transport function of the pumps and leads to a reduction in their cellular expression levels. Our observations demonstrate that ZSTK474 is a powerful anticancer drug.

Accepted manuscript

Keywords:

P-glycoprotein; ABCG2; ZSTK474; multidrug resistance; membrane transport; cancer chemotherapy

ACCEPTED MANUSCRIPT

Chemical Compounds:

ZSTK474 (PubChem CID: 11647372); vinblastine (PubChem CID: 241903); mitoxantrone (PubChem CID: 4212); calcein-AM (PubChem CID: 4126474); nicardipine (PubChem CID: 4474); fumetrimorgen C (PubChem CID: 403923)

Accepted manuscript

ACCEPTED MANUSCRIPT

1. Introduction

Chemotherapy of cancer continues to move away from geno- and cytotoxic compounds due to severe side-effects and a high susceptibility to resistance mechanisms. Components of aberrant cell signalling pathways involved in growth and proliferation provide numerous new targets. A prime candidate is the PI3K/Akt/mTOR pathway, which is up-regulated or activated in almost 50% of tumours and is involved in cell proliferation, survival and nutrient metabolism (Bauer et al., 2015; Kong and Yamori, 2008). Pharmacological inhibition of this pathway reduces cell proliferation; thereby providing the basis for potential anti-cancer activity.

Several compounds targeting the PI3K/Akt/mTOR pathway have been developed as specific inhibitors of the phosphoinositide 3-kinase (PI3K) enzyme family (Kong and Yamori, 2008). Phosphorylation of phosphatidylinositol-bisphosphate (PIP_2) generates the powerful second messenger phosphatidyl-3,4,5-trisphosphate (PIP_3), which triggers the signalling cascade involved in cell growth and survival (Engelman et al., 2006). The PI3K family comprises four classes of enzyme, each with multiple isoforms that differ in substrate specificity, tissue distribution and the downstream effectors (Vanhaesebroeck et al., 2001).

Structural data for the PI3Kγ isoform has revealed chemical features for drug binding and thereby facilitated the development of new isoform-specific inhibitors (Walker et al., 1999). One of these is the triazine derivative ZSTK474, which has been shown to inhibit the PI3K pathway in cancer cell lines and *in vivo* tumour models (Yaguchi et al., 2006). ZSTK474 inhibits cell proliferation by causing arrest of the cell cycle in the G_1-phase, but without induction of apoptosis (Dan et al., 2012; Wang et al., 2016c). ZSTK474 acts specifically on PI3K, with negligible effects on the DNA-PK and mTOR kinases (Kong and Yamori, 2008). Data gathered through a combination of pharmacological and molecular modelling approaches suggest that ZSTK474 binds to PI3K within the ATP binding pocket of the enzyme and competes at greater potency than LY294002 with nucleotide (Yaguchi et al., 2006).

Accepted manuscript

ACCEPTED MANUSCRIPT

A number of PI3K inhibitors are in clinical development and the mTOR inhibitor Everolimus has FDA approval for the treatment of renal cell carcinoma and pancreatic tumours (2016; Yao et al., 2016), and the selective PI3Kδ isoform inhibitor Idealisib has been approved as a single agent to treat small lymphocytic lymphoma and non-Hodgkin lymphoma (Nair and Cheson, 2016). Whilst these are encouraging signs for the utility of PI3K inhibitors as anticancer drugs, the spectre of resistance is ever present. A "front-line" factor in drug resistance is the over-expression of multidrug efflux pumps to mediate the ATP-dependent efflux of chemotherapy agents to levels below that required to elicit apoptosis. The efflux pumps, P-glycoprotein (P-gp, ABCB1), ABCG2 and ABCC1 (Mrp1) are from the ATP Binding Cassette (ABC) family and their over-expression is associated with a resistant phenotype and poor chemotherapeutic outcome (McHugh and Callaghan, 2008; Modok et al., 2006). This manuscript will deal specifically with ABCB1 and ABCG2, which recognise an astonishing number of substrates.

The aim of this investigation was to assess the potency and efficacy of ZSTK474 in cell lines that overexpress ABCB1 and ABCG2 to ascertain its susceptibility to these key resistance mediators.

Accepted manuscript

ACCEPTED MANUSCRIPT

2. Materials & Methods

2.1 Materials

Trypsin (Trypsin-EDTA solution), adenosine triphosphate (ATP), propidium iodide, vinblastine sulfate salt, mitoxantrone dihydrochloride, flavopiridol hydrochloride hydrate, doxorubicin hydrochloride, verapamil hydrochloride, nicardipine hydrochloride, fumitremorgin C (FTC) bortezomib, concanamycin A and calcein-acetoxy methyl ester (calcein-AM) were purchased from Sigma-Aldrich (Castle Hill, NSW). Penicillin-streptomycin solution (10000 U/ml penicillin 10000 µg/ml streptomycin) and MTT (3-(4,5-dimethylthiazol-2-yl-)-2,5-diphenyltetrazolium bromide) were purchased from ThermoFisher Scientific (Scoresby, Vic). DMEM medium was purchased from Lonza (Vic, Australia) and foetal bovine serum (FBS) from Biological Bovogen Ltd (Vic, Australia).

2.2 Tissue Culture

The drug-sensitive human breast adenocarcinoma cell line $MCF7^{WT}$ (ATCC® HTB-22™) was purchased from the American Type Culture Collection (Rockville, MD). The flavopiridol-selected ABCG2-expressing derivative cell line $MCF7^{FLV1000}$ was obtained from Dr. S Bates (National Cancer Institute, Bethesda, MD) (Robey et al., 2001) and the doxorubicin-selected ABCB1-expressing variant NCI/ADR^{Res} cell line was obtained from Dr K Cowan (National Cancer Institute, Bethesda, MD) (Mehta et al., 2002). All cell lines were grown as monolayer cultures in DMEM medium supplemented with 10% FBS, penicillin (10000 U/ml) and streptomycin (10000 mg/ml) at 37°C with 5% CO_2. To maintain selection pressure for resistance, every third passage of NCI/ADR^{Res} and $MCF7^{FLV1000}$ cells were supplemented with doxorubicin (3µM) or flavopiridol (0.5nM) respectively. All cells were maintained up to a maximum of 20 passages of sub-culture.

2.3 Cell cytotoxicity assays

Accepted manuscript

ACCEPTED MANUSCRIPT

Cytotoxicity assays were performed as previously described (Debono et al., 2014). Cells were seeded in 96-well plates at a density of 1.5 x 10^3 cells per well in 100µl medium. Cells were allowed to attach to for 24 h at 37°C and 5% CO_2. ZSTK474, anticancer drugs and pump inhibitors were added from a 2X stock solution in medium (100µl) to produce a final concentration range of 10^{-12} to 10^{-4} M. The solvent (DMSO) concentration in the wells was kept to 0.2 % (v/v). For combination cytotoxicity assays, cells were incubated with drugs as described above either in the presence of absence of ZSTK474 (0.1-3µM). Drugs and cells were incubated at 37^{o}C with 5% CO_2 for 6 days at which point the control wells (i.e. DMSO treated) had reached confluence.

The viability of cells following drug treatment was assessed using a standard MTT assay (Mosmann, 1983). Briefly, following the 6 day incubation period, 20µl of a 5mg/ml MTT solution (PBS) was added to each well, and the plates were incubated for 4 h at 37°C. Medium was aspirated and the formazan crystals dissolved in 150µl DMSO. The absorbance in each well (λ=570 nm) was measured using an iMARK 96-well plate reader and the absorbance in the control wells was assigned a value of 100%. The cytotoxic potency (IC_{50}) of each compound was determined from plots of the percentage of viable cells as a function of concentration. The data was fitted by a sigmoidal dose-response curve using GraphPad Prism® Software v6 (CA, USA).

The nature of interaction between drugs co-administered in cytotoxicity assays was evaluated by Combination Indices (CI) that were calculated using the *Lowe's Additivity Model* as described (Chou, 2006);

$$Combination\ Index = \frac{d_1}{(D_x)1} + \frac{d_2}{(D_x)2}$$

where d_1 and d_2 are the concentrations of drug needed respectively to inhibit x% of cells when used as a combination, $(D_x)_1$ is the concentration of drug 1 required to inhibit x% of cells, $(D_x)_2$ is the concentration of drug 2 needed to inhibit x% of cells.

Accepted manuscript

ACCEPTED MANUSCRIPT

For the purpose of this study, the combination indices were calculated using concentrations interpolated where the x% cells affected was 50 (IC_{50}) and 75 (IC_{75}) for the mitoxantrone/ZSTK474 combination and vinblastine/ZSTK474 combination respectively. A CI value = 1 indicates an additive effect, CI<1 indicates synergy and CI>1 indicates antagonism. It was not possible to calculate combination values with 1 and 3μM ZSTK474 combinations where the combination resulted in a cell viability of less than 20%.

2.4 The purification and functional assessment of ABCB1

ABCB1 was expressed in *Trichoplusia ni* (High-Five) cells following infection with recombinant baculovirus containing the specific mutant isoform as previously described (Taylor et al., 2001). Following infection, cells were harvested by centrifugation and the pellet stored at -80^{o}C. Crude membranes were prepared from the cells using differential ultracentrifugation following cell disruption by nitrogen cavitation as previously described (Taylor et al., 2001) and stored at -80^{o}C. ABCB1 was purified using immobilised metal affinity chromatography (IMAC) in a gravity based system, according to previously published methods with some modifications (Crowley et al., 2009; Taylor et al., 2001). The primary difference pertained to the solubilisation conditions. In the present investigation, crude membranes (30-100mg) were suspended (5mg/ml protein) in solubilisation buffer supplemented with a 0.4% (w/v) lipid mixture (4:1 ratio of *E coli* extract:cholesterol) and 2% (w/v) dodecyl-β-D-maltoside (DDM).

Accepted manuscript

Functional assessment of ABCB1 was achieved by measuring its ATPase activity based on the rate of inorganic phosphate liberation by ABCB1 containing proteoliposomes using a modified colorimetric assay (Chifflet et al., 1988; Crowley et al., 2009). In order to investigate the stimulation of ATP hydrolysis, the activity was measured as a function of added drug concentration. Proteoliposomes (0.1-0.5 μg) were incubated with ATP (2 mM) and various drug concentrations (10^{-9} to 10^{-4} M) for 40 min at 37^{o}C in 96-well plates. Once the colour-forming reaction was

ACCEPTED MANUSCRIPT

complete, the absorbance at λ=750nm was measured for all samples using an *iMark Microplate* reader. The amount of phosphate liberated was determined from extrapolation of absorbance to a standard curve of inorganic phosphate (0-20nmol P_i). In all cases the activity was expressed as moles of P_i liberated per unit time for a unit of purified ABCB1. The potency (EC_{50}) and extent of stimulation of ATPase activity (v) were estimated by non-linear regression of the general dose-response relationship to plots of activity as a function of drug concentration ([D]): $v = v_{initial} + \left(v_{final} - v_{initial}\right)/\left(1 + 10^{\left(log10(EC_{50} - [D])\right)}\right)$, where v_{initial} is the activity in the absence of drug and v_{final} is the maximal activity observed.

2.5 The calcein-AM accumulation assay in intact cells

The calcein-AM assay to measure the transport function of ABCB1 was based on a previously published method (Homolya et al., 1993). $MCF7^{WT}$ and NCI/ADR^{Res} cells were seeded into 96-well tissue culture plates at a density of 2 x 10^3 cells per well in 100µl and allowed to adhere for 2 days at 37°C with 5% CO_2. Following incubation, medium was aspirated and cells were washed with PBS and re-suspended in 100µl Hank's Buffered Salt Solution (HBSS). Test compounds (100µl) were added at a 2X final concentration in HBSS from an original stock solution of 50mM in DMSO. The final solvent (DMSO) concentration in the wells did not exceed 1% (v/v). Calcein-AM was added from a 100X HBBS stock to give a final concentration of 1µM. Following the addition of calcein-AM, plates were immediately read on a Tecan M1000 PRO plate reader using '*i control*^{TM} *1-10*' software. The plate was heated in the reader to 37°C and the fluorescence measured at an excitation λ=488nm and an emission λ=515nm. Each well was read 16 times in different locations to give an averaged fluorescence value and plates were read every minute for 10 minutes. The intracellular calcein accumulation (i.e. fluorescence intensity) was plotted as a function of time and analysed by linear regression using GraphPad Prism® Software v6. The slope of each line was used to determine the rate of calcein accumulation and plotted as a function of calcein-AM

Accepted manuscript

ACCEPTED MANUSCRIPT

concentration. These secondary plots were fitted with a hyperbolic curve using GraphPad Prism® Software v6 in order to calculate the modulator potency (MP_{50}). The MP_{50} is defined as the concentration to achieve a half-maximal calcein accumulation rate.

2.6 The flow cytometric assay for mitoxantrone accumulation

Mitoxantrone transport in whole cells by ABCG2 was measured using flow cytometry as previously described (Robey et al., 2001). $MCF7^{WT}$ and $MCF7^{FLV1000}$ cells were detached from flasks using 2mM EDTA and centrifuged at 1500*g* for 5 min, the pellet was re-suspended in PBS and re-centrifuged. The final pellet was re-suspended in HBBS in polypropylene tubes at a density of 10^6 cells/ml. Cells were incubated in (i) HBSS alone, (ii) HBSS with 3µM mitoxantrone or (iii) HBSS in the presence of 5µM mitoxantrone in combination with ZSTK474 (1-100µM) for 1h at 37°C on a Stuart SB2 Rotator. Stock solutions of all compounds were prepared in DMSO and the final concentration of DMSO did not exceed 1% (v/v), which was determined not to affect mitoxantrone accumulation (Mahringer et al., 2009). Cells were centrifuged twice at 2000*g* for 8 minutes at 4°C using an Allegra X-12R centrifuge, re-suspended in 500µl ice-cold HBSS solution and transferred to cluster tubes. The centrifugation step was repeated, supernatant removed and 100µl of HBSS was added to the pellet. A BD Scientific LSR-II Flow Cytometer with a red 633 nm laser was used to detect mitoxantrone fluorescence and doublet discrimination was achieved by gating forward-scatter versus side-scatter. Dead cells were excluded using propidium iodide (PI) staining (1µg/ml) detected using the blue 488 nm laser. The PI was added immediately prior to flow cytometry analysis. A minimum of ten thousand events were collected per sample and the data was processed using FlowJo Software (OR, USA). Data was represented as a histogram showing mean intracellular mitoxantrone accumulation in the absence or presence of test compound using GraphPad Prism® Software v6.

Accepted manuscript

ACCEPTED MANUSCRIPT

2.7 Protein levels in MCF7^{WT}, MCF7^{FLV1000} and NCI/ADR^{Res} cell lines

Cells were seeded in sterile flat-bottomed 6-well tissue culture plates at 5 x 10^4 cells per well and allowed to attach to the surface for 24 h at 37°C 5% CO_2. Following 24 h incubation, a "time zero" (or untreated) sample was obtained by aspirating medium from one well, washing with PBS and lysing with 1% (w/v) SDS. The test compound, at concentrations indicated in the figure legends, was added to the remaining five wells. All drugs were prepared from a 50mM DMSO stock solution and the final DMSO concentration did not exceed 1% (v/v). Lysates were prepared from treated cells every day for 4 days following drug addition and a final sample was taken 6 days after treatment. The cell lysates were stored at -20°C until use.

Cell lysates were sheared with a fine gauge needle and the total protein concentration of each sample was determined using the Detergent Compatible BioRad assay using BSA as a standard. Samples of lysate were subjected to SDS-PAGE and transferred to Amersham™ Protran™ Nitrocellulose Membranes (GE Healthcare Lifesciences, NSW, Australia). The mouse monoclonal C219 antibody (Sapphire Bioscience) was used to specifically detect ABCB1 and mouse monoclonal BXP-21 antibody (ThermoFisher, Vic, Australia) was used to detect ABCG2. A secondary antibody, Amersham™ ECL sheep anti-mouse IgG peroxidase-linked whole antibody (GE Healthcare, NSW, Australia), was used to detect bound antibody using chemi-luminescence with the Amersham™ ECL Western Blotting Detection Kit (GE Healthcare, NSW, Australia). Immuno-reactive protein bands were visualised on the GelDoc Vilber Fusion SL Chemi-luminescence System.

Normalisation of the 8% SDS-PAGE gels was achieved quantitatively by loading 9μg of total cellular protein in each lane. This strategy of equi-loading based on protein amount obviates the potential for erroneous loading with house-keeping genes due to the myriad cellular effects of drug treatments used in this investigation (Farmer et al., 1983; Gorr and Vogel, 2015).

Accepted manuscript

ACCEPTED MANUSCRIPT

2.8 Quantitative measurement of ABCB1 and ABCG2 mRNA levels

NCI/ADR^{Res} & MCF7^{FLV1000} cells were seeded at a density of 10^5 per well in duplicate and left to attach overnight at 37^{o}C incubator with 5% CO_2. Cells were treated with ZSTK474 (1μM) or solvent (DMSO) control for a total of 4 days, with samples collected every 24 h. Following incubation, the cells were washed in sterile PBS and total RNA extracted using the NucleoSpin® RNA extraction kit (MACHEREY-NAGEL) according to the manufacturer's protocol. RNA concentration and purity was determined using a Nanodrop ND-1000 spectrophotometer (Thermo Fisher). Preparations of RNA were treated with a DNAse (1U, 30min, 37^{o}C) to remove any contaminating DNA. RNA (1μg) was reverse transcribed for 1h at 50^{o}C using the Superscript III Kit (Invitrogen, Life Technologies) using random hexamers (Promega) and the cDNA was stored at -80^{o}C until further use.

Primers for target (ABCB1 & ABCG2) and the housekeeping gene GAPDH were designed using the NCBI primer blast database (http://www.ncbi.nlm.nih.gov/tools/primer-blast). Primers, where possible, spanned an exon-exon boundary region with primer size kept restricted to 18-22 bases with predicted amplicon sizes of 70 to 150bp. The melting temperature range was 58 to 62^{o}C and GC content was maintained at 20-60%. The primer sequences are shown in Table 1 and were purchased from Geneworks (Hindmarsh, Australia). Primers were re-suspended in nuclease free water and stored at -20^{0}C.

Cellular ABCB1 and ABCG2 mRNA levels were measured using qRT-PCR in 96-well plates. The reaction mixture (20μl) comprised of cDNA template, a final concentration of 300nM forward and reverse primers, and Fast SYBR Green Master Mix (Applied Biosystems). Samples were run on the Applied Biosystems StepOne Real-Time PCR system with 40 cycles of denaturation, annealing and extension. The relative expression of the target gene (ABCB1 and ABCG2) was calculated relative to GAPDH using the comparative (ΔΔCt) method.

Accepted manuscript

ACCEPTED MANUSCRIPT

2.9 Quantitative measurement of protein synthesis – the effects of ZSTK474

$MCF7^{WT}$, NCI/ADR^{Res} and $MCF7^{FLV1000}$ cells were seeded into black (clear bottom) 96 well plates at a density of 2.5 x 10^4 cells per well and left to attach overnight in a 37^0C incubator with 5% CO_2. After 24 h the cells were treated with either (a) ZSTK474 (1-3μM) for 48 h, or, (b) cyclohexamide (100μg/ml) pre-incubated with the cells for one hour. The effects of drug treatment on total cellular protein synthesis were determined using the Protein Synthesis Assay Kit purchased from Cayman Chemicals (Michigan, USA). The rate of protein synthesis, compared to a no treatment control, was measured using a TECAN M100PRO plate reader to record fluorescence according to the manufacturer's protocol. The relative percentage of protein synthesis was calculated using the equation: $\% \, protein \, synthesis = \left(\frac{RFU \, of \, treated \, well}{RFU \, of \, untreated \, well}\right) \times 100$.

2.10 Data analysis

All curve-fitting and statistical analyses of data were carried out using GraphPad Prism® Software v6. The Student's t test was used for statistical analyses of two groups and for comparison of three or more groups, a one-way analysis of variance (ANOVA) using the Dunnett's post-hoc test was used to compare values. P-values of <0.05 were considered statistically significant.

Accepted manuscript

ACCEPTED MANUSCRIPT

3. Results

3.1 Anti-proliferative activity of ZSTK474 in human cancer cell lines expressing ABCB1 & ABCG2

$MCF7^{WT}$, $MCF7^{FLV1000}$ and NCI/ADR^{Res} cell lines were incubated in the presence of ZSTK474 (10^{-12} to 10^{-4}M) for a period of six days and the percentage of live cells remaining was measured (Fig. 1). In the parental $MCF7^{WT}$ cell line, the potency of ZSTK474 was defined as IC_{50} = 0.13±0.02μM (n=7) and the number of live cells was <5% at 100μM. ZSTK474 also produced growth inhibition of the ABCG2-expressing $MCF7^{FLV1000}$ cells with a potency (IC_{50} = 0.19±0.05μM, n=7) that was not significantly different to the MCF7 cells. In contrast, the potency of ZSTK474 in NCI/ADR^{Res} cells, which over-express ABCB1, was reduced to IC_{50} = 1.70±0.31μM (n=7). This 13-fold reduction in ZSTK474 potency was statistically significant ($P<0.05$) but modest in comparison to the degree of resistance observed for vinblastine (see below).

3.2 Effects of ZSTK474 in combination with vinblastine on growth inhibition

The cytotoxicity of vinblastine was measured in the presence of ZSTK474 (0.1 to 3μM) in both $MCF7^{WT}$ (Fig. 2a) and NCI/ADR^{Res} (Fig. 2c) cell lines to assess the possibility of a potentiated effect with the two drugs. The cytotoxic potency for vinblastine in $MCF7^{WT}$ cells was characterised by IC_{50} = 0.20±0.07nM and the addition of ZSTK474 generated a downward shift in the initial plateau level of the cytotoxicity profile (Fig. 2a). In the presence of 0.1μM ZSTK474, the cytotoxicity of vinblastine displayed a lower initial plateau (54±12% live cells) but no change in potency (IC_{50} = 0.16±0.07nM). At higher ZSTK474 concentrations, the reduction in the initial plateau level was even greater with only 17±9% remaining at 3μM.

The cytotoxicity of vinblastine in NCI/ADR^{Res} cells was characterised by an IC_{50} = 181±80nM, which is 905-fold lower than in $MCF7^{WT}$ cells. Co-addition of ZSTK474 (0.3μM) to NCI/ADR^{Res} cells caused the apparent potency of vinblastine to increase three-fold, to an IC_{50} value of 63±19nM

Accepted manuscript

ACCEPTED MANUSCRIPT

(Fig. 2c). The potency was further increased (IC_{50} = 19±8nM) at the highest ZSTK474 concentration (3μM), which was 9-fold lower than observed with vinblastine alone. The co-addition of ZSTK474 also caused a downward shift in the initial plateau of the dose-response curves. For example, the initial plateau at 0.1μM ZSTK474 was maintained at 96±5% live cells and at 3μM this was reduced to 69±10%. Clearly, the reduction in the initial plateau was not as pronounced as observed in the $MCF7^{WT}$ cells. However, the increase in the apparent vinblastine potency was only observed in the resistant NCI/ADR^{Res} cells.

To ascertain whether the enhanced response was an additive or synergistic interaction, the data were evaluated using combination index (CI) analysis. The CI was determined at each concentration of ZSTK474 co-administered with vinblastine and the values are shown in Fig. 3(a-b). An effect level that produced a 75% reduction in live cells was selected for analysis. The 75% level was chosen due to the effect of ZSTK474 on the initial plateau level. The CI values (for 0.1 and 0.3μM ZSTK474) in the $MCF7^{WT}$ cells were not significantly different from a value of 1.0 based on analysis of the 95% confidence interval, which is suggestive of an additive effect. The large reduction in the initial plateau level at higher concentrations precluded determination of a CI value. In contrast, the CI values determined in the NCI/ADR^{Res} cells at each ZSTK474 concentration were significantly lower than the isobole (dotted lines Fig. 3). This indicates that the combination of vinblastine and ZSTK474 exerts a synergistic effect, specifically in the ABCB1 expressing NCI/ADR^{Res} cells.

Accepted manuscript

3.3 Effects of ZSTK474 in combination with mitoxantrone on growth inhibition

Interaction between ZSTK4747 and the anticancer drug mitoxantrone was also investigated in $MCF7^{WT}$ and the ABCG2-expressing $MCF7^{FLV1000}$ cell lines (Fig. 2 (b,d)). The potency of mitoxantrone in drug sensitive $MCF7^{WT}$ cells was characterised by an IC_{50} of 21±6nM in the absence of PI3K inhibitor (Fig. 2b). The apparent mitoxantrone potency was increased by the addition of 0.1μM (IC_{50} = 8.9±2.3nM) and 0.3μM (IC_{50} = 4.1±0.9nM) ZSTK474; the latter

ACCEPTED MANUSCRIPT

represents a statistically significant ($P<0.05$) increase from the control value. The initial plateau level for mitoxantrone in the presence of 0.1μM ZSTK474 was reduced to 76±12% live cells and further reduced to 51±18% at 0.3μM. Higher ZSTK474 concentrations resulted in less than 25% live $MCF7^{WT}$ cells, thereby preventing the assignment of an accurate IC_{50}-value.

The $MCF7^{FLV1000}$ cells displayed 420-fold resistance to mitoxantrone as shown by the significant reduction in potency (IC_{50} = 8777±380nM) (Fig. 2d) compared to the $MCF7^{WT}$ cells (IC_{50} = 21±6nM) (Fig. 2b). In the presence of 0.3μM ZSTK474, the potency of mitoxantrone was increased 9-fold (IC_{50} = 959±426nM). At higher concentrations of ZSTK474 resulted in the reduction of the live cell population to <25% of the original level, similar to that observed in $MCF7^{WT}$ cells.

The interaction between mitoxantrone and ZSTK474 was assessed using CI analysis as shown in Fig. 3 (c-d). The CI values at 0.3μM were not significantly different from the isobole (dotted line; CI=1.0) and indicate an additive effect of the two drugs. At the lowest concentration of ZSTK474 (0.1μM) there was clear evidence of a synergistic interaction, although this occurred in both cell lines and was therefore independent of ABCG2. Unfortunately, the extent of reduction in the initial plateau level at ZSTK474 concentrations of 1-3μM prevented assignment of a CI value in either cell line.

Accepted manuscript

3.4 The effects of ZSTK474 on the drug transport and ATP hydrolysis functions of ABCB1

The ability of ZSTK474 to alter the transport activity of ABCB1 was investigated with the calcein-AM accumulation assay (Homolya et al., 1993). Calcein-AM and various concentrations of ZSTK474 (or nicardipine) were added to $MCF7^{WT}$ and NCI/ADR^{Res} cells and the fluorescence intensity measured for ten minutes.

As expected (Homolya et al., 1993), the addition of either ZSTK474, or nicardipine, failed to cause any alteration in the rate of calcein-AM accumulation in the $MCF7^{WT}$ cell line. The rates of fluorescence accumulation in NCI/ADR^{Res} cells were plotted as a function of drug concentration as

ACCEPTED MANUSCRIPT

shown for nicardipine (Fig. 4a). The data was fitted by a hyperbolic function to enable estimation of the maximal rate of fluorescence increase (ΔF_{MAX}) and the modulator potency (MP_{50}) to achieve this increase. The ΔF_{MAX} in the presence of nicardipine was 110±19 r.f.u/min (n=11) with a potency defined as MP_{50} = 2.5±0.6μM. ZSTK474 also caused a significant increase in fluorescent signal in NCI/ADR^{Res} cells as shown in Fig. 4b. The ΔF_{MAX} was 20±4 r.f.u/min (n=5) in the presence of ZSTK474 and the potency to achieve this rate was MP_{50} = 1.7±0.5μM. Therefore, ZSTK474 is able to modulate the transport function of ABCB1 in NCI/ADR^{Res} cells in a manner similar to nicardipine, which suggests a direct interaction between the drug and ABCB1.

The effects of ZSTK474 on the activity of purified, reconstituted ABCB1 were used to ascertain whether there was a direct drug-protein interaction. The ability to stimulate (or inhibit) ATP hydrolysis by ABCB1 is a standard measure to indicate interaction with the transporter. As shown in Fig. 5, ZSTK474 caused a concentration dependent increase in the rate of ATP hydrolysis by ABCB1. The basal ATPase activity was V_{MIN} = 239±69 nmol Pi/min/mg and this was stimulated 4.5±0.9-fold by ZSTK474 to a maximal activity of 831±177 nmol Pi/min/mg. The potency of ZSTK474 to stimulate ATP hydrolysis was defined with an EC_{50} value of 7.6±1.7μM. Nicardipine also stimulated the basal activity (V_{MIN} = 98±45 nmol Pi/min/mg) by 5.3±0.7-fold to a maximal activity of V_{MAX} = 591±99 nmol Pi/min/mg. Furthermore, nicardipine stimulated ATP hydrolysis by ABCB1 with a similar potency (EC_{50} = 6.5±1.8μM) to ZSTK474, which is in agreement with previously published values (Crowley et al., 2009).

Together, these data indicate that ZSTK474 modulates the transport function of ABCB1 in a similar manner to nicardipine. Moreover, this modulation occurs via a direct interaction with the transporter based on its ability to stimulate ATP hydrolysis by ABCB1.

3.5 The effects of ZSTK474 on mitoxantrone accumulation in ABCG2 expressing cells

Accepted manuscript

ACCEPTED MANUSCRIPT

The ability of ZSTK474 to modulate the function of ABCG2 was also investigated given the overlap in substrate specificity with ABCB1. The ABCG2 substrate mitoxantrone is intrinsically fluorescent and a flow cytometry assay was used to measure its steady-state accumulation in $MCF7^{WT}$ and $MCF7^{FLV1000}$ cells.

Fig. 6a shows representative data for mitoxantrone accumulation of in both cell lines. In $MCF7^{WT}$ cells mitoxantrone accumulation ($3.3x10^4$ r.f.u) was 2.6-fold greater than that observed in the drug-resistant $MCF7^{FLV1000}$ cells ($1.25x10^4$ r.f.u). Furthermore, the addition of the ABCG2 inhibitor FTC (10μM) to $MCF7^{FLV1000}$ cells resulted in a 2.3-fold increase in mitoxantrone accumulation ($2.9x10^4$ r.f.u). In contrast, FTC addition to $MCF7^{WT}$ cells did not result in any appreciable change in fluorescence ($3.5x10^4$ r.f.u) (*data not shown for clarity*).

Fig. 6b shows the effects of ZSTK474 on the extent of mitoxantrone accumulation in both $MCF7^{WT}$ and $MCF7^{FLV1000}$ cell lines. In the absence of ZSTK474, $MCF7^{WT}$ cells (39,368±6,744 r.f.u) accumulated 4.1-fold more mitoxantrone than the $MCF7^{FLV1000}$ cells (9,476±1,680 r.f.u). The addition of ZSTK474 did not alter mitoxantrone accumulation in $MCF7^{WT}$ cells. In contrast, ZSTK474 produced a concentration dependent increase in mitoxantrone accumulation, with a 2.2-fold increase at 100μM (21,2976±3,550 r.f.u) in $MCF7^{FLV1000}$ cells. This compares similarly to the 2.4-fold increase in mitoxantrone accumulation produced by the ABCG2 inhibitor FTC (50μM), which reached 22,989±1,451 r.f.u (*data not shown*). The data demonstrate that ZSTK474 is able to modulate substrate transport by ABCG2 to a similar extent as FTC.

Accepted manuscript

3.6 The effects of ZSTK474 on ABCB1 expression in cancer cell lines

Data described in preceding sections demonstrated that ZSTK474 could directly modulate the transport activity of ABCB1 and ABCG2. However, ZSTK474 modulates many cellular functions controlled by the PI3K/Akt pathway and may therefore have additional influences on ABCB1 and ABCG2 expression.

ACCEPTED MANUSCRIPT

ABCB1 expression levels in lysates from NCI/ADR^{Res} cells showed a gradual increase in the first 2-3 days, before reaching a plateau (Fig. 7a). In the presence of ZSTK474 (1μM), the cellular levels of ABCB1 were unaffected in the first two days. However, in subsequent days the expression of ABCB1 decreased. The expression blots were repeated multiple times (n>3) and ZSTK474 reproducibly caused a reduction in ABCB1 levels (6233±2232 vs 13941±2729 pixels). In contrast to ZSTK474, the addition of nicardipine (1μM) had no effect on ABCB1 expression in NCI/ADR^{Res} cells (Fig. 7b).

The effects of both drugs on cellular levels of the essential membrane protein Na/K-ATPase were also investigated. ZSTK474 caused a significant, time-dependent reduction in expression of the Na/K-ATPase in both NCI/ADR^{Res} (Fig. 7c) and MCF7^{WT} cells (Fig. 7e). Nicardipine, however, did not cause any change in Na/K-ATPase levels in NCI/ADR^{Res} cells (Fig. 7d). The data with the Na/K-ATPase suggests that ZSTK474 may have a general effect on cellular protein levels.

Since ABCB1 is degraded through the proteasomal pathway, the effects of ZSTK474 on ABCB1 expression were assessed in the presence, and absence, of the proteasome inhibitor Bortezomib. As shown in Fig. 9a, expression of ABCB1 reached plateau on day 4 at which time ZSTK474 (1μM) was added (marked with arrow). The 2-day incubation with ZSTK474 was sufficient to reduce ABCB1 levels (10,780±760 vs 15,930±3377 pixels). On the other hand, bortezomib had no significant effect on ABCB1 levels (Fig. 9b). However, the co-administration of bortezomib and ZSTK474 led to diminution of ABCB1 expression (2466±601 vs 15930±3377 pixels) at day 6 (Fig. 9c). The lack of any stabilisation of ABCB1 levels during co-addition with bortezomib suggests that ZSTK474 does not influence ABCB1 levels by enhancing its proteasomal degradation. In addition, the inability of bortezomib treatment to increase ABCB1 expression may be related to the ability of this pump to mediate efflux of the proteasomal inhibitor (O'Connor et al., 2013).

Altered transcription provides an alternative mechanism for ZSTK474 to modulate ABCB1 expression. Consequently, ABCB1 mRNA levels were measured using qRT-PCR and related to the

Accepted manuscript

ACCEPTED MANUSCRIPT

house-keeping gene GAPDH, whose mRNA levels were unaffected by ZSTK474 (1μM). ABCB1 mRNA levels at 24-hour post-seeding, obtained in the absence of ZSTK474, were normalised to a value of 1.0 (Fig. 10a). In the subsequent 72-hour period, cells were incubated with ZSTK474 (1μM) and ABCB1 mRNA levels measured every 24-hours. As shown in Fig. 10a, the addition of ZSTK474 to the NCI/ADR^{Res} cells did not alter ABCB1 mRNA levels over 72-hours. This suggests that the observed reduction in ABCB1 expression by ZSTK474 was unlikely to have occurred through altered transcription.

Steady-state levels of proteins also depend on the rate of *de novo* synthesis. Consequently, the effects of ZSTK474 on total cellular protein synthesis were measured using a fluorescent assay involving O-propargyl-puromycin (OPP), which incorporates into the C-terminus of nascent polypeptide and halts translation. OPP contains an alkyne moiety that reacts with the carboxy-fluorescein containing FAM-azide; thereby enabling its detection by fluorescence spectroscopy. Fig. 11 shows the effects of ZSTK474 or cycloheximide on total protein synthesis. The translation inhibitor cycloheximide (100μg/ml) was used as a positive control as shown by reduction in *de novo* protein synthesis in the MCF7^{WT} cells to 42±8% and to 53±10% in the NCI/ADR^{Res} cells. At 3μM, ZSTK474 reduced overall protein synthesis in the NCI/ADR^{Res} cells to 62±5% ($P<0.05$) of the untreated sample and to 49±5% ($P<0.05$) in the MCF7^{WT} cells. At both concentrations investigated, ZSTK474 caused a significant reduction in overall protein synthesis in drug sensitive and resistant cells. This reduction in overall cellular protein synthesis may result in lower levels of ABCB1 in NCI/ADR^{Res} cells and also account for reduced levels of Na/K-ATPase in both cell lines.

Accepted manuscript

3.7 The effects of ZSTK474 on the levels of ABCG2 in cancer cell lines

During a 6-day growth period, levels of ABCG2 reached a plateau approximately 2-3 days post-seeding of MCF7^{FLV1000} cells (Fig. 8a). In the presence of ZSTK474 (1μM), the levels of ABCG2 were similar to the vehicle control for the first 48 hours. However, the levels of ABCG2 decreased

ACCEPTED MANUSCRIPT

dramatically (5196±899 vs 14285±2976 pixels) by day 6 in the presence of ZSTK474 (Fig. 8a). In contrast, the ABCG2 inhibitor FTC (1μM) had no appreciable effect on ABCG2 levels in $MCF7^{FLV1000}$ cells (Fig. 8b). Therefore, the reduction in ABCG2 expression caused by ZSTK474 was not simply related to prolonged inhibition of ABCG2 function.

The effects of ZSTK474 on Na/K-ATPase levels were also measured over the 6-day growth period in $MCF7^{FLV1000}$ cells (Fig. 8c). The addition of ZSTK474 (1μM) resulted in reduced levels of Na/K-ATPase in the cells, suggesting a general effect on cellular proteins. In contrast, addition of FTC (1μM) did not cause any alteration in Na/K-ATPase levels in $MCF7^{FLV1000}$ cells.

The primary cellular degradation pathway for ABCG2 is lysosomal. ZSTK474 (1μM) produced a reduction in ABCG2 levels compared to the vehicle control in $MCF7^{FLV1000}$ cells (Fig. 9d). In contrast, the lysosomal inhibitor concanamycin A had no appreciable effect on ABCG2 levels (Fig. 9e). However, the combination of ZSTK474 and concanamycin A produced an increase in ABCG2 levels (Fig. 9f). The ability of concanamycin A to prevent the ZSTK474-mediated reduction in ABCG2 expression suggests an involvement of the lysosomal degradation route.

The possibility that ZSTK474 alters ABCG2 levels by reducing transcription was also investigated using a similar treatment strategy to that described for ABCB1 (Fig. 10b). Incubation (24-96 h) of $MCF7^{FLV1000}$ cells with ZSTK474 (1μM) did not cause a statistically significant alteration in ABCG2 mRNA levels, indicating that transcription was unaffected.

The effects of ZSTK474 on protein translation in cells expressing ABCG2 were also undertaken using the OPP-based fluorescent assay and the results are shown in Fig. 11. Addition of ZSTK474 (1μM) was associated with reduced protein translation to 66±8 % ($P<0.05$) compared to untreated $MCF7^{FLV1000}$ cells. Increasing the concentration of ZSTK474 to 3μM did not produce any further reduction, with protein translation maintained at 67±4% of control. This decrease in the *de novo* protein synthesis by ZSTK474 accounts for the reduction in ABCG2 levels in the $MCF7^{FLV1000}$ cell line.

Accepted manuscript

ACCEPTED MANUSCRIPT

Accepted manuscript

ACCEPTED MANUSCRIPT

4. Discussion

The majority of compounds developed to circumvent ABCB1 or ABCG2 mediated resistance are classified as "inhibitors" that prevent drug efflux and restore anticancer drug accumulation to levels that inhibit cell proliferation. Despite success *in vitro*, this has failed to translate into clinical usage and alternative strategies are clearly required. The PI3K inhibitor ZSTK474 offers numerous advantages over previously described ABCB1/ABCG2 inhibitors. Specifically, this investigation has shown that ZSTK474 (i) inhibits drug transport by ABCB1 and ABCG2, (ii) reduces levels of the pumps and (iii) possesses inherent anti-proliferative activity.

The anti-proliferative activity of ZSTK474 has also been demonstrated in numerous cell lines and xenograft models (Yaguchi et al., 2006; Zhou et al., 2016), resulting in cell cycle arrest in G1-phase (Kong and Yamori, 2008). Cell cycle arrest is related to modulating the PI3K/Akt signalling pathway. In the present investigation, the growth inhibitory effects of ZSTK474 in breast cancer cells were unaffected by the presence of ABCB1 or ABCG2. Moreover, the growth arrest by ZSTK474 was synergistic when co-administered with vinblastine in cells expressing ABCB1. This synergy may be related to the cellular target of vinblastine, which is a disruptor of microtubule mass and dynamics. Synergy also exists between ZSTK474 and the Bcr-Abl inhibitor Imatinib in the chronic myelogenous leukaemia (CML) cell line K562 (Zhou et al., 2016). Co-administration of ZSTK474 also improved the cytotoxic potency of Imatinib in the drug resistant variant K562/A02, which over-expresses ABCB1. The authors concluded that ZSTK474 was able to "overcome" the ABCB1 mediated resistance against Imatinib. It is possible that ZSTK474 may either inhibit ABCB1, or that it "competes" for transport out of the cells with vinblastine and thereby exhibits synergistic activity.

An analogous situation was observed in resistant cells that over-express ABCG2 where the addition of ZSTK474 potentiated the cytotoxicity of mitoxantrone; in this case the interaction was additive. This potentiation agrees with an earlier investigation demonstrating that the PI3K/Akt inhibitor

Accepted manuscript

ACCEPTED MANUSCRIPT

LY294002 could also overcome the resistance phenotype conferred by ABCG2 to the topoisomerase-I inhibitors SN-38 and topotecan (Imai et al., 2012). Moreover, ABCG2 did not confer resistance to LY294002 *per se*. In contrast, ABCG2 was able to confer resistance to another PI3K inhibitor CUDC-907 by reducing its intracellular accumulation (Wu et al., 2016). In the present investigation, ABCG2 over-expression did not lead to resistance of cells to the anti-proliferative activity of ZSTK474, which suggests that it is not a substrate for transport by this pump. In addition, a recent study has shown that exposure of cells to ZSTK474 for over a year failed to generate elevated levels of ABCG2 (Isoyama et al., 2012).

The observation that the anti-proliferative activity of ZSTK474 is unaffected by the presence of ABCB1, or ABCG2, does not preclude a direct interaction between ZSTK474 and either pump. The addition of ZSTK474 rapidly produced an increase in the accumulation of calcein-AM in ABCB1 expressing cells. The rapidity of this effect suggests a direct action on the transport process. In the case of ABCG2, ZSTK474 also inhibited transport of mitoxantrone with similar potency to the ABCG2-selective inhibitor FTC and over a comparable timeframe. A direct interaction has been reported for another PI3K inhibitor, LY294002 (Pick and Wiese, 2012). Therefore it appears that ZSTK474, whilst not a substrate for transport by the pumps, is able to overcome the drug resistant phenotype conferred by ABCB1 or ABCG2 via direct inhibition of their transport activity.

Corroborating evidence of a direct ZSTK474-protein interaction was obtained using purified reconstituted ABCB1. The rate of ATP hydrolysis by ABCB1 was stimulated by ZSTK474 to a similar extent and potency to that observed for the inhibitor nicardipine. Numerous studies have demonstrated that the direct binding of inhibitors and substrates to ABCB1 produce altered rates of ATP hydrolysis (Wang et al., 2012). For example, the inhibitor Tariquidar reduces the rate of ATP hydrolysis, whereas inhibitors such as nicardipine are associated with stimulatory effects (Zhang et al., 2008). It has been postulated that inhibitors of transport may actually stimulate ATP hydrolysis by uncoupling drug binding from nucleotide hydrolysis during translocation (Nair and Cheson,

Accepted manuscript

ACCEPTED MANUSCRIPT

2016). Data from the present investigation indicates that ZSTK474 can directly interact with ABCB1 and this interaction is likely responsible for the reduction in calcein-AM efflux.

ZSTK474 has been predicted by molecular modelling to bind within the ATP-binding pocket of PI3K to produce inhibition of kinase activity (Yaguchi et al., 2006). However, it is unlikely to interact within the Nucleotide Binding Domains (NBDs) of ABCB1, which provide energy for transport. The primary reason was the observation that ZSTK474 stimulates the rate of ATP hydrolysis by ABCB1. It is established that ABCB1 requires two fully functional NBDs to carry-out ATP hydrolysis and subsequent drug translocation (Urbatsch et al., 1995). Binding of the compound to either, or both, NBDs would preclude ATP hydrolysis by ABCB1 and therefore, ZSTK474 is more likely to exert its effect by interaction at the poly-specific drug binding cavity in the transmembrane domain.

It is possible that inhibition of the PI3K/Akt signalling pathway by ZSTK474 may also influence the resistance conferred by ABCB1 or ABCG2 via indirect effects. Both 3-methyl-adenine (Zou et al., 2014) and the Traditional Chinese Medicine formulation Zuo Jin Wan (Sui et al., 2014) have been shown to restore anticancer drug potency in cells expressing ABCB1 by inhibiting the PI3K/Akt/mTOR pathway. Similarly, siRNA and pharmacological approaches to inhibiting PI3K/Akt signalling have resulted in reduced levels of ABCG2 and restoration of anticancer drug sensitivity (Komeili-Movahhed et al., 2015; Takada et al., 2005). These reports implicate the PI3K/Akt pathway in regulating the resistance phenotype conferred by these efflux pumps with an indirect mechanism, such as a reduction in their expression.

In the present investigation, ZSTK474 also caused a significant reduction in the expression of ABCB1 in the NCI/ADR^{Res} cells. This did not occur through transcriptional regulation since the levels of mRNA for ABCB1 were unaltered by drug. Furthermore, ZSTK474 did not enhance ABCB1 degradation since inhibition of the proteasome by bortezomib would have been anticipated to elevate ABCB1 levels. Strikingly, co-administration of bortezomib with ZSTK474 produced a

Accepted manuscript

ACCEPTED MANUSCRIPT

synergistic reduction in ABCB1 levels. This may be explained by a bortezomib mediated reduction in ABCB1 expression in certain cell lines by modulating the NF-κB pathway (Wang et al., 2012). Another widely used proteasome inhibitor, MG-1302, also causes a reduction in ABCB1 expression via interaction with Bcl-2 (Zhang et al., 2008). These observations render attribution of a proteasomal mechanism to the ZSTK474-mediated reduction in ABCB1 expression problematic.

ZSTK474 also caused a marked reduction in ABCG2 levels in $MCF7^{FLV1000}$ cells. Unlike ABCB1, the degradation of ABCG2 occurs through the lysosomal pathway (Wakabayashi et al., 2007). Several xanthines have been shown to reduce expression of ABCG2, and overcome chemo-resistance, by enhancing its degradation in the lysosome (Ding et al., 2012). However, the co-addition of ZSTK474 with the lysosomal inhibitor concanamycin A resulted in only minor elevation of ABCG2 expression. This suggests that the ZSTK474 uses an alternative pathway to reduce levels of ABCG2.

The observation that ZSTK474 also caused reduced levels of Na^+/K^+-ATPase in drug sensitive and resistant cells offered the possibility of a more generic effect. This idea was supported by the large decrease in the overall cellular rate of protein translation caused by ZSTK474 in all three cell lines. The PI3K/Akt signalling pathway has myriad cellular effects with altered protein expression typically occurring through the route involving mTOR (Bauer et al., 2015; Kong and Yamori, 2008). Moreover, it has been shown in neuronal tissue that ZSTK474 leads to specific inhibition of the mTORC1 pathway (Wang et al., 2016b), which is normally involved in the activation of protein translation processes. Inhibition of the Akt/mTOR signalling pathway by compounds such as resveratrol will lead to decreased protein synthesis, including ABCB1 as shown in drug resistant K562/ADR cells (Wang et al., 2016a). Furthermore, the resveratrol-mediated reduction in ABCB1 expression restored the sensitivity of K562/ADR cells to the anti-proliferative di-peptide Bestatin. Similarly, blocking the PI3K/Akt/mTOR signalling pathway by 3-methyl-adenine has been shown to reduce levels of ABCG2 and sensitise cells to a variety of anticancer drugs (Zou et al., 2014).

Accepted manuscript

ACCEPTED MANUSCRIPT

Together these observations support the conclusion that inactivation of the PI3K/Akt/mTOR pathway by ZSTK474 has an indirect effect on the resistant phenotype, namely, the reduction in ABCB1 and ABCG2 through inhibition of overall protein translation.

Conclusions: We have shown that the PI3K inhibitor ZSTK474 causes multiple effects on drug resistant cancer cells that over-express the efflux pumps ABCB1 and ABCG2. ZSTK474 causes growth inhibition in resistant and sensitive cells with similar potency, suggesting that its accumulation is relatively unaffected by these two pumps. Nonetheless, ZSTK474 can restore anticancer drug efficacy in resistant cell lines, which was achieved by directly inhibiting the drug transport activity of the pumps. ZSTK474 also facilitated the activity of anticancer drugs by reducing levels of ABCB1 or ABCG2 through a post-transcriptional mechanism. Therefore, ZSTK474 offers a novel multi-pronged strategy to restore anticancer drug efficacy in cells expressing ABCB1 or ABCG2. These observations warrant further investigation into combination therapy, particularly in tumours exhibiting over-expression of these multidrug efflux pumps.

Accepted manuscript

ACCEPTED MANUSCRIPT

References

2016. FDA Approves Drug Combo for Kidney Cancer. Cancer Discov 6, 687-688.

Bauer, T.M., Patel, M.R., Infante, J.R., 2015. Targeting PI3 kinase in cancer. Pharmacol Ther 146, 53-60.

Chifflet, S., Chiesa, U.T.R., Tolosa, S., 1988. A method for the determination of inorganic phosphate in the presence of labile organic phosphate and high concentrations of protein: application to lens ATPases. Anal. Biochem. 168, 1-4.

Chou, T.C., 2006. Theoretical basis, experimental design, and computerized simulation of synergism and antagonism in drug combination studies. Pharmacol Rev 58, 621-681.

Crowley, E., O'Mara, M.L., Reynolds, C., Tieleman, D.P., Storm, J., Kerr, I.D., Callaghan, R., 2009. Transmembrane helix 12 modulates progression of the ATP catalytic cycle in ABCB1. Biochemistry 48, 6249-6258.

Dan, S., Okamura, M., Mukai, Y., Yoshimi, H., Inoue, Y., Hanyu, A., Sakaue-Sawano, A., Imamura, T., Miyawaki, A., Yamori, T., 2012. ZSTK474, a specific phosphatidylinositol 3-kinase inhibitor, induces G1 arrest of the cell cycle in vivo. Eur J Cancer 48, 936-943.

Debono, A.J., Mistry, S.J., Xie, J., Muthiah, D., Phillips, J., Ventura, S., Callaghan, R., Pouton, C.W., Capuano, B., Scammells, P.J., 2014. The synthesis and biological evaluation of multifunctionalised derivatives of noscapine as cytotoxic agents. ChemMedChem 9, 399-410.

Ding, R., Shi, J., Pabon, K., Scotto, K.W., 2012. Xanthines down-regulate the drug transporter ABCG2 and reverse multidrug resistance. Mol Pharmacol 81, 328-337.

Engelman, J.A., Luo, J., Cantley, L.C., 2006. The evolution of phosphatidylinositol 3-kinases as regulators of growth and metabolism. Nat Rev Genet 7, 606-619.

Farmer, S.R., Wan, K.M., Ben-Ze'ev, A., Penman, S., 1983. Regulation of actin mRNA levels and translation responds to changes in cell configuration. Mol Cell Biol 3, 182-189.

Gorr, T.A., Vogel, J., 2015. Western blotting revisited: critical perusal of underappreciated technical issues. Proteomics Clin Appl 9, 396-405.

Homolya, L., Hollo, Z., Germann, U.A., Pastan, I., Gottesman, M.M., Sarkadi, B., 1993. Fluorescent cellular indicators are extruded by the multidrug resistance protein. J Biol Chem 268, 21493-21496.

Imai, Y., Yoshimori, M., Fukuda, K., Yamagishi, H., Ueda, Y., 2012. The PI3K/Akt inhibitor LY294002 reverses BCRP-mediated drug resistance without affecting BCRP translocation. Oncol Rep 27, 1703-1709.

Isoyama, S., Dan, S., Nishimura, Y., Nakamura, N., Kajiwara, G., Seki, M., Irimura, T., Yamori, T., 2012. Establishment of phosphatidylinositol 3-kinase inhibitor-resistant cancer cell lines and therapeutic strategies for overcoming the resistance. Cancer Sci 103, 1955-1960.

Komeili-Movahhed, T., Fouladdel, S., Barzegar, E., Atashpour, S., Hossein Ghahremani, M., Nasser Ostad, S., Madjd, Z., Azizi, E., 2015. PI3K/Akt inhibition and down-regulation of BCRP re-sensitize MCF7 breast cancer cell line to mitoxantrone chemotherapy. Iran J Basic Med Sci 18, 472-477.

Accepted manuscript

ACCEPTED MANUSCRIPT

Kong, D., Yamori, T., 2008. Phosphatidylinositol 3-kinase inhibitors: promising drug candidates for cancer therapy. Cancer Sci 99, 1734-1740.

Mahringer, A., Delzer, J., Fricker, G., 2009. A fluorescence-based in vitro assay for drug interactions with breast cancer resistance protein (BCRP, ABCG2). Eur J Pharm Biopharm 72, 605-613.

McHugh, K., Callaghan, R., 2008. Clinical trials on MDR reversal agents, in: Colabufo, N.A. (Ed.), Multidrug Resistance: Biological and Pharmaceutical Advances in Antitumour Treatment. Research Signpost, Kerala, pp. 321-353.

Mehta, K., Devarajan, E., Chen, J., Multani, A., Pathak, S., 2002. Multidrug-Resistant MCF-7 Cells: An Identity Crisis? Journal of the National Cancer Institute 94, 1652-1654.

Modok, S., Mellor, H.R., Callaghan, R., 2006. Modulation of multidrug resistance efflux pump activity to overcome chemoresistance in cancer. Curr Opin Pharmacol 6, 350-354.

Mosmann, T., 1983. Rapid colorimetric assay for cellular growth and survival: application to proliferation and cytotoxicity assays. J Immunol Methods 65, 55-63.

Nair, K.S., Cheson, B., 2016. The role of idelalisib in the treatment of relapsed and refractory chronic lymphocytic leukemia. Ther Adv Hematol 7, 69-84.

O'Connor, R., Ooi, M.G., Meiller, J., Jakubikova, J., Klippel, S., Delmore, J., Richardson, P., Anderson, K., Clynes, M., Mitsiades, C.S., O'Gorman, P., 2013. The interaction of bortezomib with multidrug transporters: implications for therapeutic applications in advanced multiple myeloma and other neoplasias. Cancer Chemother Pharmacol 71, 1357-1368.

Pick, A., Wiese, M., 2012. Tyrosine kinase inhibitors influence ABCG2 expression in EGFR-positive MDCK BCRP cells via the PI3K/Akt signaling pathway. ChemMedChem 7, 650-662.

Robey, R.W., Medina-Perez, W.Y., Nishiyama, K., Lahusen, T., Miyake, K., Litman, T., Senderowicz, A.M., Ross, D.D., Bates, S.E., 2001. Overexpression of the ATP-binding cassette half-transporter, ABCG2 (Mxr/BCrp/ABCP1), in flavopiridol-resistant human breast cancer cells. Clin Cancer Res 7, 145-152.

Sui, H., Pan, S.F., Feng, Y., Jin, B.H., Liu, X., Zhou, L.H., Hou, F.G., Wang, W.H., Fu, X.L., Han, Z.F., Ren, J.L., Shi, X.L., Zhu, H.R., Li, Q., 2014. Zuo Jin Wan reverses P-gp-mediated drug-resistance by inhibiting activation of the PI3K/Akt/NF-kappaB pathway. BMC Complement Altern Med 14, 279.

Takada, T., Suzuki, H., Gotoh, Y., Sugiyama, Y., 2005. Regulation of the cell surface expression of human BCRP/ABCG2 by the phosphorylation state of Akt in polarized cells. Drug Metab Dispos 33, 905-909.

Taylor, A.M., Storm, J., Soceneantu, L., Linton, K.J., Gabriel, M., Martin, C., Woodhouse, J., Blott, E., Higgins, C.F., Callaghan, R., 2001. Detailed characterization of cysteine-less P-glycoprotein reveals subtle pharmacological differences in function from wild-type protein. Br J Pharmacol 134, 1609-1618.

Urbatsch, I.L., Sankaran, B., Bhagat, S., Senior, A.E., 1995. Both P-glycoprotein nucleotide-binding sites are catalytically active. J Biol Chem 270, 26956-26961.

Vanhaesebroeck, B., Leevers, S.J., Ahmadi, K., Timms, J., Katso, R., Driscoll, P.C., Woscholski, R., Parker, P.J., Waterfield, M.D., 2001. Synthesis and function of 3-phosphorylated inositol lipids. Annu Rev Biochem 70, 535-602.

Accepted manuscript

ACCEPTED MANUSCRIPT

Wakabayashi, K., Nakagawa, H., Tamura, A., Koshiba, S., Hoshijima, K., Komada, M., Ishikawa, T., 2007. Intramolecular disulfide bond is a critical check point determining degradative fates of ATP-binding cassette (ABC) transporter ABCG2 protein. J Biol Chem 282, 27841-27846.

Walker, E.H., Perisic, O., Ried, C., Stephens, L., Williams, R.L., 1999. Structural insights into phosphoinositide 3-kinase catalysis and signalling. Nature 402, 313-320.

Wang, H., Wang, X., Li, Y., Liao, A., Fu, B., Pan, H., Liu, Z., Yang, W., 2012. The proteasome inhibitor bortezomib reverses P-glycoprotein-mediated leukemia multi-drug resistance through the NF-kappaB pathway. Pharmazie 67, 187-192.

Wang, L., Wang, C., Jia, Y., Liu, Z., Shu, X., Liu, K., 2016a. Resveratrol Increases Anti-Proliferative Activity of Bestatin Through Downregulating P-Glycoprotein Expression Via Inhibiting PI3K/Akt/mTOR Pathway in K562/ADR Cells. J Cell Biochem 117, 1233-1239.

Wang, P., He, Y., Li, D., Han, R., Liu, G., Kong, D., Hao, J., 2016b. Class I PI3K inhibitor ZSTK474 mediates a shift in microglial/macrophage phenotype and inhibits inflammatory response in mice with cerebral ischemia/reperfusion injury. J Neuroinflammation 13, 192.

Wang, Y., Liu, J., Qiu, Y., Jin, M., Chen, X., Fan, G., Wang, R., Kong, D., 2016c. ZSTK474, a specific class I phosphatidylinositol 3-kinase inhibitor, induces G1 arrest and autophagy in human breast cancer MCF-7 cells. Oncotarget 7, 19897-19909.

Wu, C.P., Hsieh, Y.J., Hsiao, S.H., Su, C.Y., Li, Y.Q., Huang, Y.H., Huang, C.W., Hsieh, C.H., Yu, J.S., Wu, Y.S., 2016. Human ATP-Binding Cassette Transporter ABCG2 Confers Resistance to CUDC-907, a Dual Inhibitor of Histone Deacetylase and Phosphatidylinositol 3-Kinase. Mol Pharm 13, 784-794.

Yaguchi, S., Fukui, Y., Koshimizu, I., Yoshimi, H., Matsuno, T., Gouda, H., Hirono, S., Yamazaki, K., Yamori, T., 2006. Antitumor activity of ZSTK474, a new phosphatidylinositol 3-kinase inhibitor. J Natl Cancer Inst 98, 545-556.

Yao, J.C., Fazio, N., Singh, S., Buzzoni, R., Carnaghi, C., Wolin, E., Tomasek, J., Raderer, M., Lahner, H., Voi, M., Pacaud, L.B., Rouyrre, N., Sachs, C., Valle, J.W., Delle Fave, G., Van Cutsem, E., Tesselaar, M., Shimada, Y., Oh, D.Y., Strosberg, J., Kulke, M.H., Pavel, M.E., 2016. Everolimus for the treatment of advanced, non-functional neuroendocrine tumours of the lung or gastrointestinal tract (RADIANT-4): a randomised, placebo-controlled, phase 3 study. Lancet 387, 968-977.

Zhang, Y., Shi, Y., Li, X., Du, R., Luo, G., Xia, L., Du, W., Chen, B., Zhai, H., Wu, K., Fan, D., 2008. Proteasome inhibitor MG132 reverses multidrug resistance of gastric cancer through enhancing apoptosis and inhibiting P-gp. Cancer Biol Ther 7, 540-546.

Zhou, Q., Chen, Y., Chen, X., Zhao, W., Zhong, Y., Wang, R., Jin, M., Qiu, Y., Kong, D., 2016. In Vitro Antileukemia Activity of ZSTK474 on K562 and Multidrug Resistant K562/A02 Cells. Int J Biol Sci 12, 631-638.

Zou, Z., Zhang, J., Zhang, H., Liu, H., Li, Z., Cheng, D., Chen, J., Liu, L., Ni, M., Zhang, Y., Yao, J., Zhou, J., Fu, J., Liang, Y., 2014. 3-Methyladenine can depress drug efflux transporters via blocking the PI3K-AKT-mTOR pathway thus sensitizing MDR cancer to chemotherapy. J Drug Target 22, 839-848.

Accepted manuscript

ACCEPTED MANUSCRIPT

Acknowledgements

The work in this manuscript was generously supported by a project grant (#12-0008) from Worldwide Cancer Research. The authors wish to thank Dr Amee George (John Curtin School of Medical Research, ANU) for her advice on the qRT-PCR assay.

Author Contributions

Muthiah – All experimental aspects of the project and assistance with writing

Callaghan – Project design, co-ordination and manuscript writing

Conflict Of Interest

The authors declare that they have no conflicts of interest with the contents of this article.

Accepted manuscript

ACCEPTED MANUSCRIPT

Figure Legends

Figure 1 Cytotoxicity of ZSTK474 in cells over-expressing ABCB1 and ABCG2

$MCF7^{WT}$ (●), NCI/ADR^{Res} (❍) and $MCF7^{FLV1000}$ (■) cells were grown in the presence of ZSTK474 (10^{-12} to 10^{-4} M) for seven days. The percentage of viable cells remaining after this time was determined using an MTT assay. The data shown as mean±S.E.M was fitted by the general dose-response relationship using non-linear regression and was obtained from a minimum of three independent observations.

Figure 2 Potentiation of anticancer drug cytotoxicity by ZSTK474 in cells expressing ABCB1 or ABCG2

Cell cytotoxicity was determined for anticancer drugs in the presence of varying concentrations ZSTK474 (none ●; 0.1μM ■; 0.3μM ▲; 1μM ▼; 3μM ◆) for seven days. Dose response curves were generated in $MCF7^{WT}$ (a) and NCI/ADR^{Res} cells (c) using vinblastine (10^{-11} to 10^{-4} M). Mitoxantrone (10^{-11} to 10^{-3} M) was used in $MCF7^{WT}$ (b) and $MCF7^{FLV1000}$ (d) cells. The data was fitted by the general dose-response relationship using non-linear regression. Secondary plots were generated to show the extent of cell death obtained at a 10^{-11} M concentration of vinblastine (e) or mitoxantrone (f) in the presence of varying ZSTK474 concentrations for sensitive (*filled bars*) and resistant cells (*clear bars*). All data represent the mean±S.E.M obtained from a minimum of three independent observations.

Figure 3 Isobologram analyses of cytotoxicity profiles of vinblastine/ZSTK474 and mitoxantrone/ZSTK474 combinations in $MCF7^{WT}$, NCI/ADR^{Res} and $MCF7^{FLV1000}$ cells

Accepted manuscript

ACCEPTED MANUSCRIPT

Combination Index values for the vinblastine/ZSTK474 combination in (a) $MCF7^{WT}$ and (b) NCI/ADR^{Res} cells were determined from IC_{75} values. Combination Index values for the mitoxantrone/ZSTK474 combination in (c) $MCF7^{WT}$ and (d) $MCF7^{FLV1000}$ cells were calculated at 50% cell death (IC_{50}). The line of additivity is shown as a dotted line; points below the dotted line indicate synergy, points on the line indicate an additive effect and points above the line indicate antagonism. Values shown are the average ± S.E.M from ≥3 independent experiments.

Figure 4 ***The effects of ZSTK474 and nicardipine on calcein-AM accumulation in cells over-expressing ABCB1***

$MCF7^{WT}$ and NCI/ADR^{Res} cells were grown to confluency in 96-well plates and calcein-AM (2μM) was added in the presence or absence of drug. Fluorescence was measured for a period of 10 minutes following the addition of calcein-AM and the rate determined from the slope of the change in fluorescence. The rate of calcein-AM accumulation was plotted as a function of either (a) nicardipine or (b) ZSTK474 and fitted, by non-linear regression, with a hyperbolic function. Data represents the mean±S.E.M obtained from at least three independent observations.

Figure 5 ***Stimulation of the ATPase activity of purified, reconstituted P-gp by ZSTK474***

Purified, reconstituted P-gp was incubated in the presence of a fixed concentration of ATP (2mM) and varying concentrations of ZSTK474. The samples were incubated at 37°C for 40 minutes and the amount of inorganic phosphate liberated was determined using a colorimetric assay. ATPase activity was normalised for protein amount and plotted as a function of ZSTK474 concentration. The general dose-response relationship was fitted using non-linear regression and the data represents the mean±S.E.M obtained from four independent observations.

Accepted manuscript

ACCEPTED MANUSCRIPT

Figure 6 ***The effects of ZSTK474 on mitoxantrone accumulation in cells over-expressing ABCG2***

The effect of ZSTK474 on the transport process of ABCG2 was measured using a flow cytometry assay. $MCF7^{WT}$ and $MCF7^{FLV1000}$ cells were incubated for an hour with mitoxantrone (3μM) in the presence or absence of varying concentrations of ZSTK474 and the intracellular accumulation of mitoxantrone was detected using a BD LSR II flow cytometer equipped with a red 633 nm laser.

(a) Cell count was plotted as a function of the average mitoxantrone accumulation in $MCF7^{WT}$ cells (*red solid line*), $MCF7^{FLV1000}$ cells (*blue solid line*) and $MCF7^{FLV1000}$ cells in the presence of 10μM ZSTK474 (*dotted blue line*).

(b) A histogram was generated for mitoxantrone accumulation in $MCF7^{WT}$ (*clear bars*) and $MCF7^{FLV1000}$ (*solid bars*) cells the presence of increasing ZSTK474 concentrations. Data represents the mean±S.E.M obtained from at least three independent observations. * indicates a statistically significant ($P<0.05$) difference from the value obtained in $MCF7^{FLV1000}$ cells in the absence of ZSTK474.

Figure 7 ***Effects of ZSTK474 and nicardipine on ABCB1 and Na/K-ATPase levels in NCI/ADR^{Res} cells***

$MCF7^{WT}$ and NCI/ADR^{Res} cells were incubated withZSTK474 (1μM) or nicardipine (1μM) for up to 6 days. Lysates were prepared in 1% (w/v) SDS and the total protein concentration was determined for each sample. The expression of ABCB1 (140kD band) was detected using the C219 monoclonal antibody and the Na/K-ATPase α-subunit (100kD band) detected with the C464.6 monoclonal antibody. Each panel provides a representative vehicle control (DMSO) and the drug treatment. ABCB1 expression in NCI/ADR^{Res} cells was shown in panels (a) and (b) following treatment with ZSTK474 and nicardipine, respectively. Na/K-ATPase levels in NCI/ADR^{Res} cells

Accepted manuscript

ACCEPTED MANUSCRIPT

are shown in panels (c) and (d) following treatment with ZSTK474 and nicardipine respectively. Panel (e) shows the expression of Na/K-ATPase in the absence or presence of ZSTK474 in $MCF7^{WT}$ cells. Normalisation of the 8% SDS-PAGE gels was achieved quantitatively by loading 9μg of total cellular protein in each lane.

Figure 8 ***Effect of ZSTK474 and FTC on ABCG2 and Na/K-ATPase levels in $MCF7^{FLV1000}$ cells***

ZSTK474 (1μM) or FTC (1μM) were added to $MCF7^{WT}$ and $MCF7^{FLV1000}$ cells for a period of 6 days. Lysates were prepared in 1% (w/v) SDS, the protein concentration was determined and 9μg of total cellular protein in each lane of an 8% SDS-PAGE gel. The expression of ABCG2 was detected (72kD band) using the BXP-21 monoclonal antibody and the Na/K-ATPase α-subunit (100kD band) with the monoclonal antibody C464.6. The blot in each panel consists of samples obtained from either a vehicle control (DMSO) or the drug treatment. ABCG2 levels in $MCF7^{FLV1000}$ cells are shown in panels (a) and (b) following treatment with ZSTK474 and FTC respectively. Na/K-ATPase levels in $MCF7^{FLV1000}$ cells are shown in panels (c) and (d) following treatment with ZSTK474 and FTC, respectively.

Accepted manuscript

Figure 9 ***Effects of ZSTK474 and protein degradation pathway inhibitors on ABCB1 and ABCG2***

ZSTK474 was added to drug cells alone or in combination with inhibitors of protein degradation. Drugs, inhibitors or vehicle (DMSO) were added at day four (↑), when ABCB1 or ABGC2 expression reached steady-state and left for a further two days. Lysates were prepared in 1% (w/v) SDS, the total protein concentration was determined for each sample and 9μg loaded in each lane. ABCB1 (140kD band) was detected in NCI/ADR^{Res} cells (NCI) using the monoclonal antibody

ACCEPTED MANUSCRIPT

C219 and ABCG2 (72kD band) was detected in MCF7^{FLV1000} cells (FLV) using the monoclonal antibody BXP-21. Bortezomib (BZ) (10nM) was used to inhibit proteasomal degradation and concanamycin A (ConA) (50nM) was used to inhibit lysosomal protein degradation.

Figure 10 Effects of ZSTK474 on ABCB1 and ABCG2 mRNA levels

NCI/ADR^{Res} (a) or MCF7^{FLV1000} cells (b) were treated with ZSTK474 (1μM) for four days. Samples were collected every 24 hours and mRNA levels for the two transporters measured by qRT-PCR. ABCB1 and ABCG2 mRNA levels were normalised relative to GAPDH. The latter was assigned a value of 1.0 and the data represent the mean±S.E.M obtained from three independent observations.

Figure 11 The effects of ZSTK474 on de novo protein synthesis in MCF7^{WT}, NCI/ADR^{Res} and MCF7^{FLV1000} cells

MCF7^{WT} and NCI/ADR^{RES} cells were incubated in the presence or absence of ZSTK474 or cyclohexamide for 24 hours. In the MCF7^{FLV1000} cell line, the incubation with ZSTK474 was extended to 48 hours. Total *de novo* protein synthesis was measured using a fluorescence based assay that detects incorporation of a puromycin analogue OPP. The clear, black and hashed bars represent relative protein synthesis in MCF7^{WT}, NCI/ADR^{RES} and MCF7^{FLV1000} cells, respectively. Values were normalised relative to the no drug control, which was set to an arbitrary value of 100%. Data shown were obtained from at least three independent observations. * indicates a statistically significant ($P<0.05$) difference compared to the value obtained for each cell line in the absence of added drug using one way ANOVA.

Accepted manuscript

ACCEPTED MANUSCRIPT

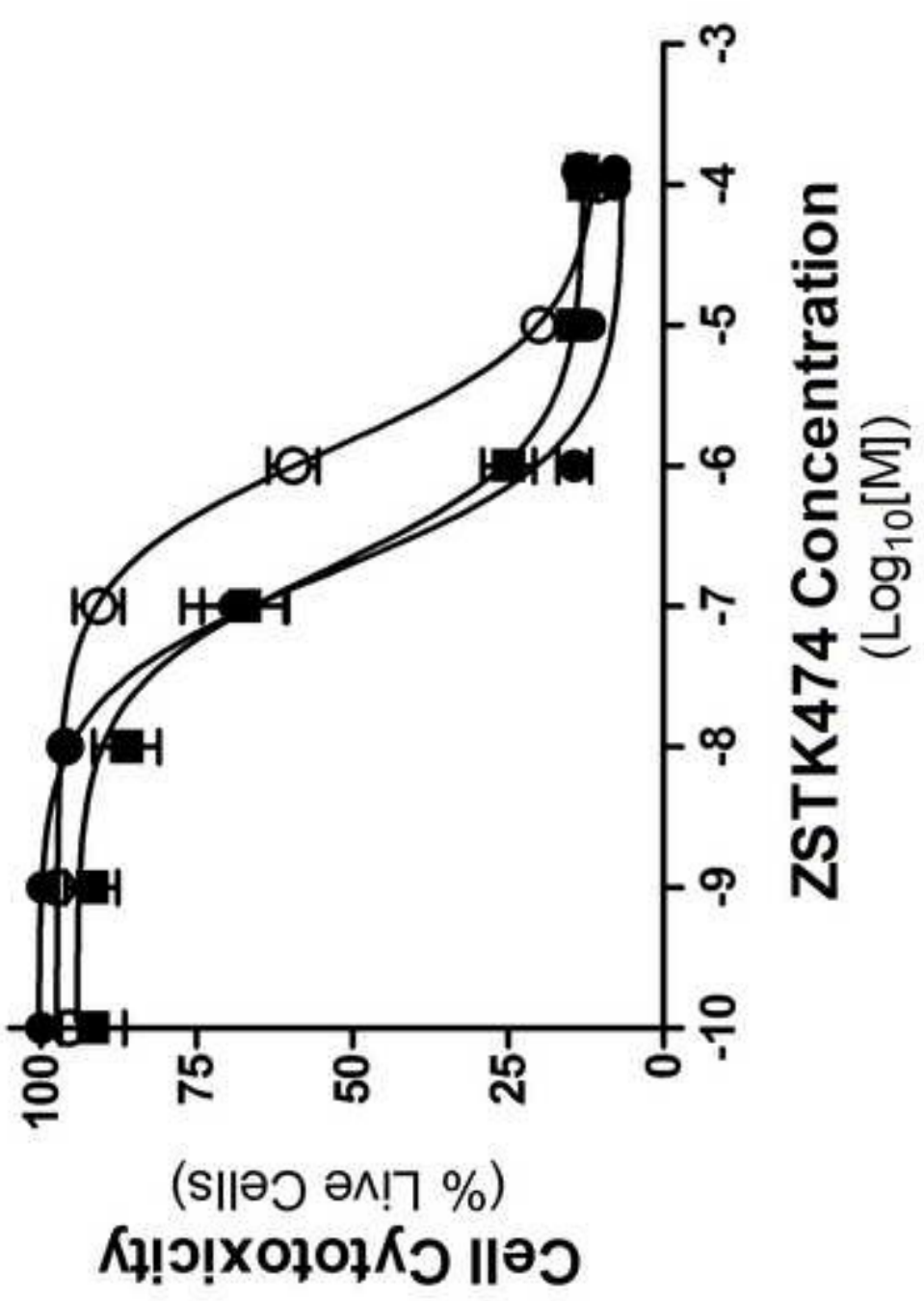

FIGURE 1

Figure 1

Figure 2

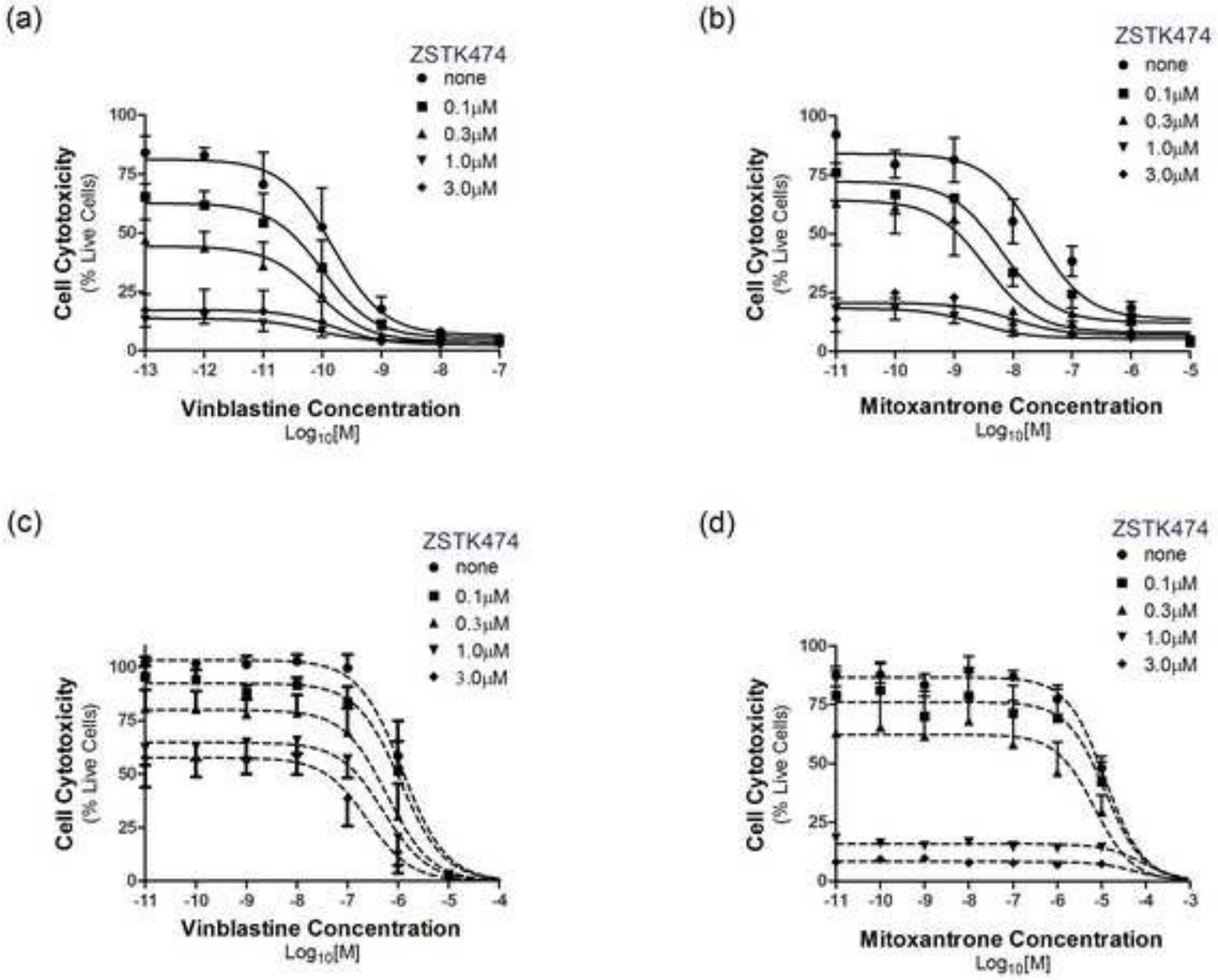

ACCEPTED MANUSCRIPT

FIGURE 2

Figure 3

FIGURE 3

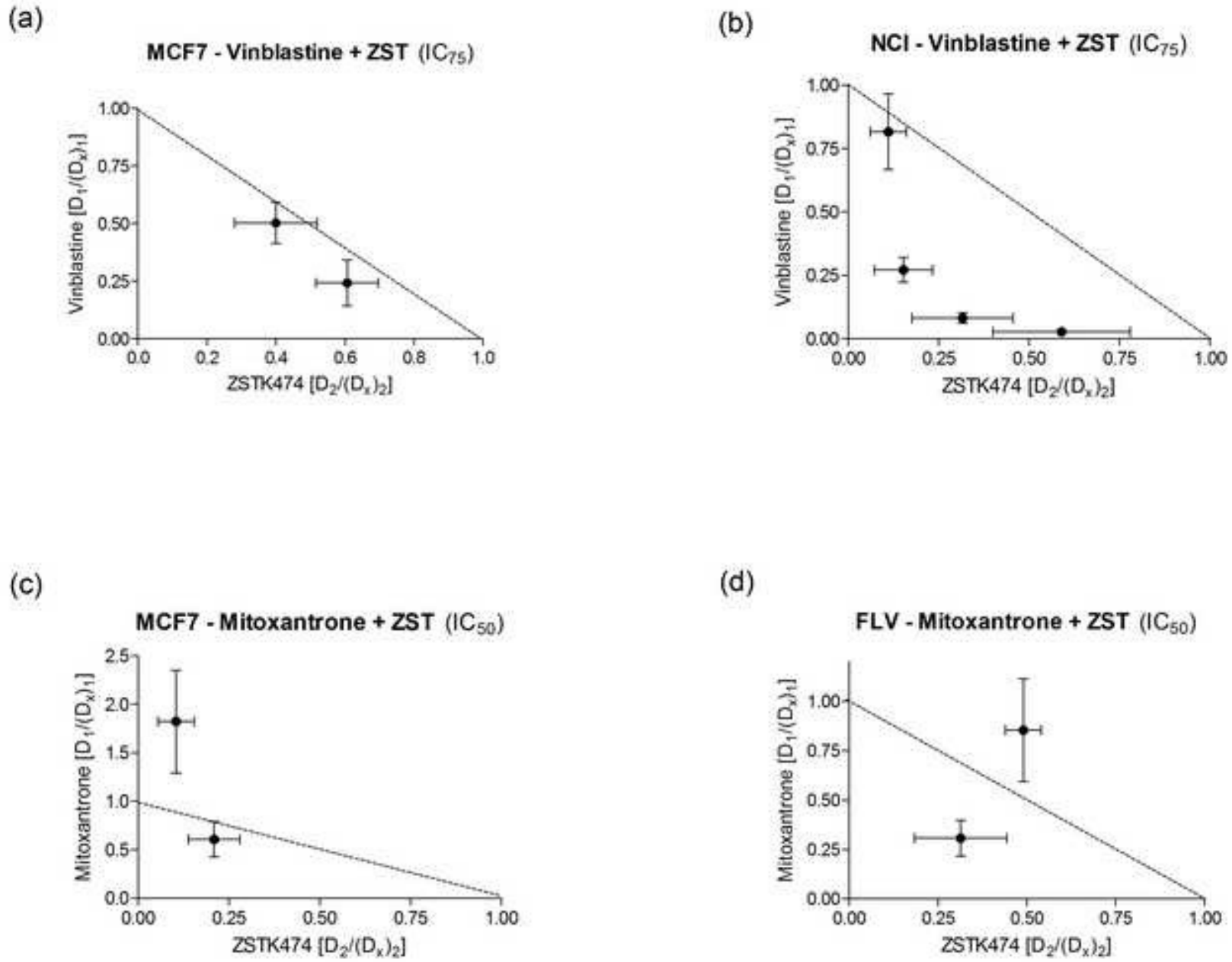

ACCEPTED MANUSCRIPT

Figure 4

ACCEPTED MANUSCRIPT

(a)

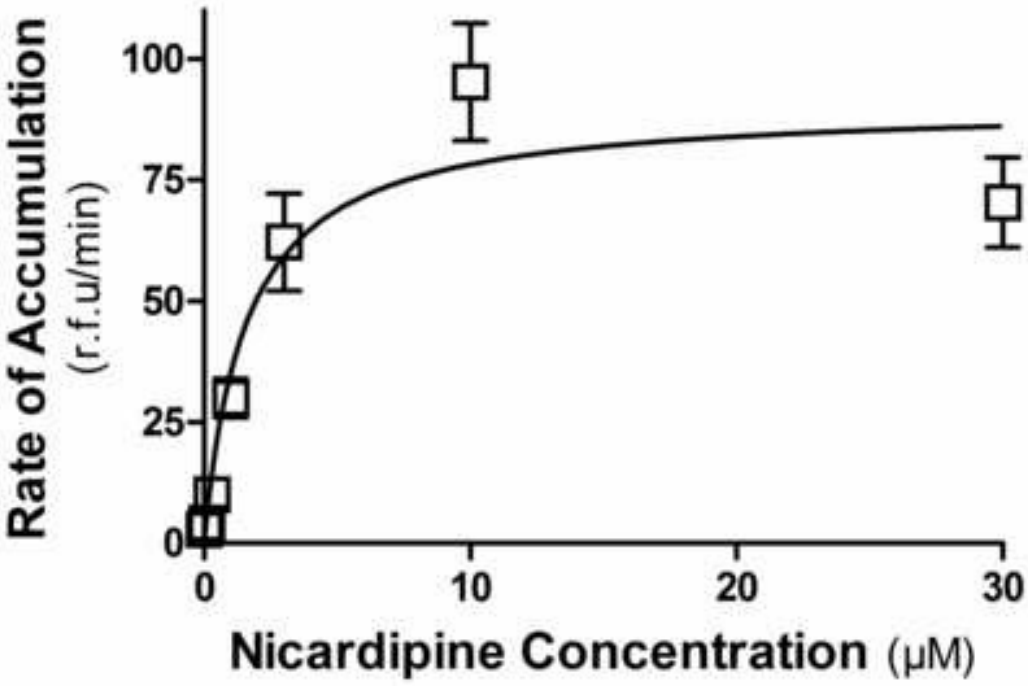

(b)

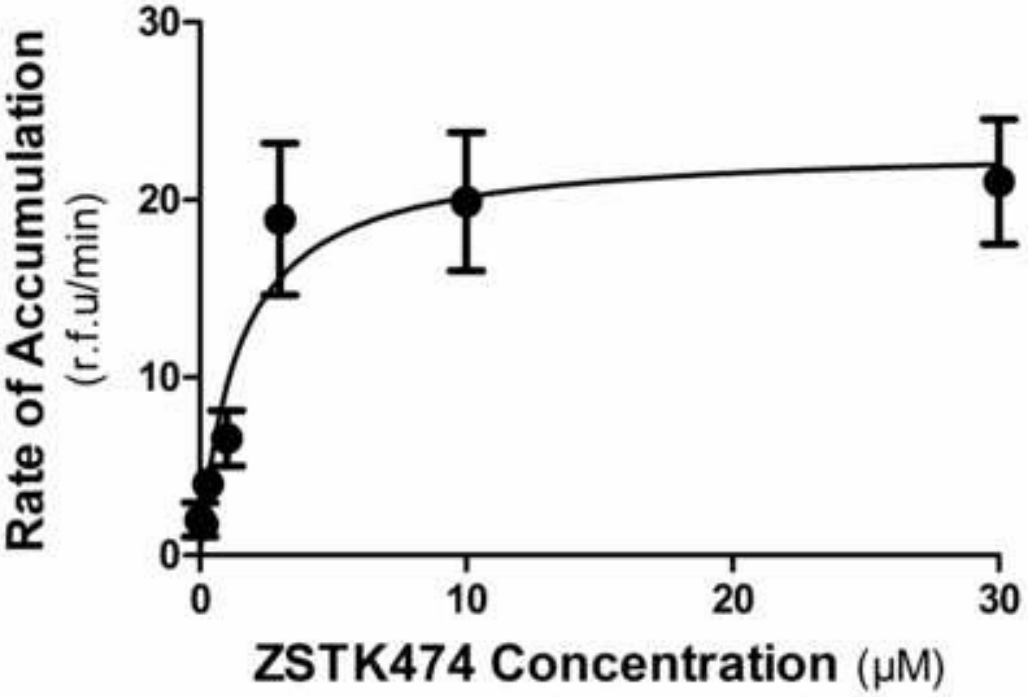

FIGURE 4

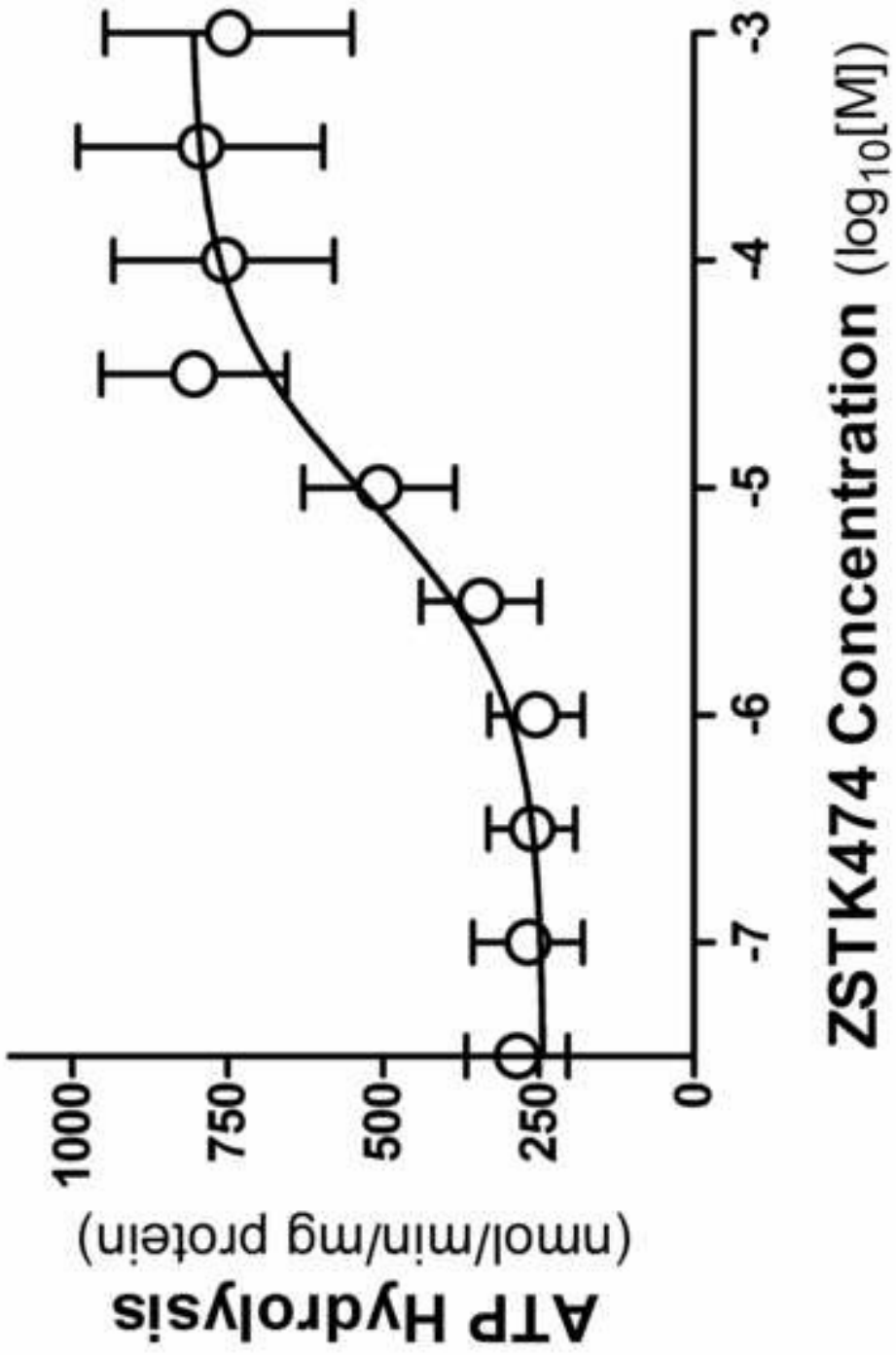

FIGURE 5

Figure 5

Figure 6

ACCEPTED MANUSCRIPT

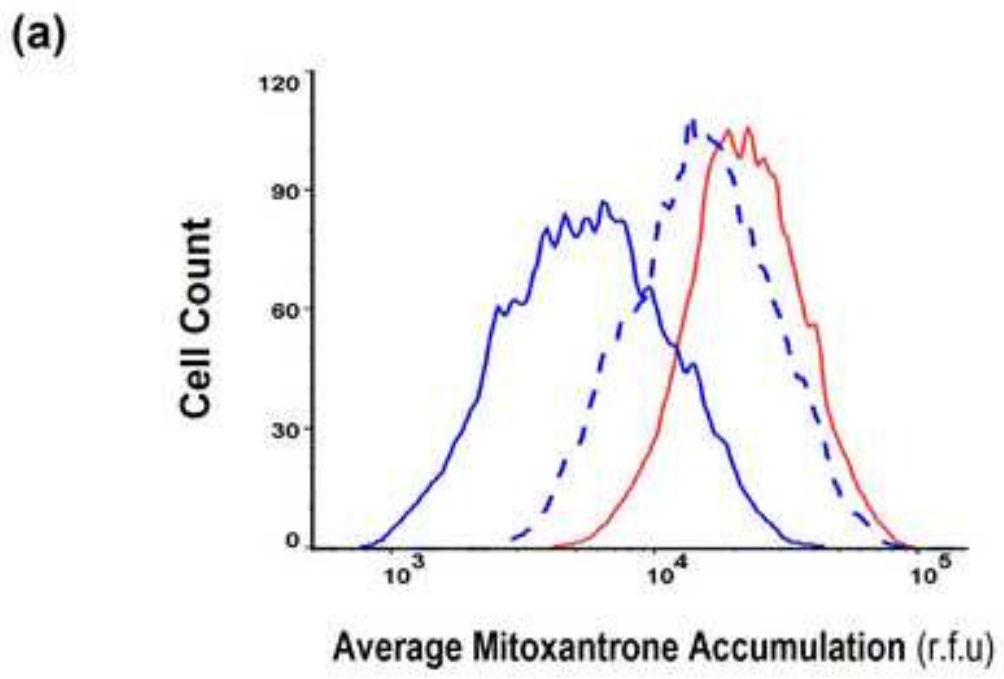

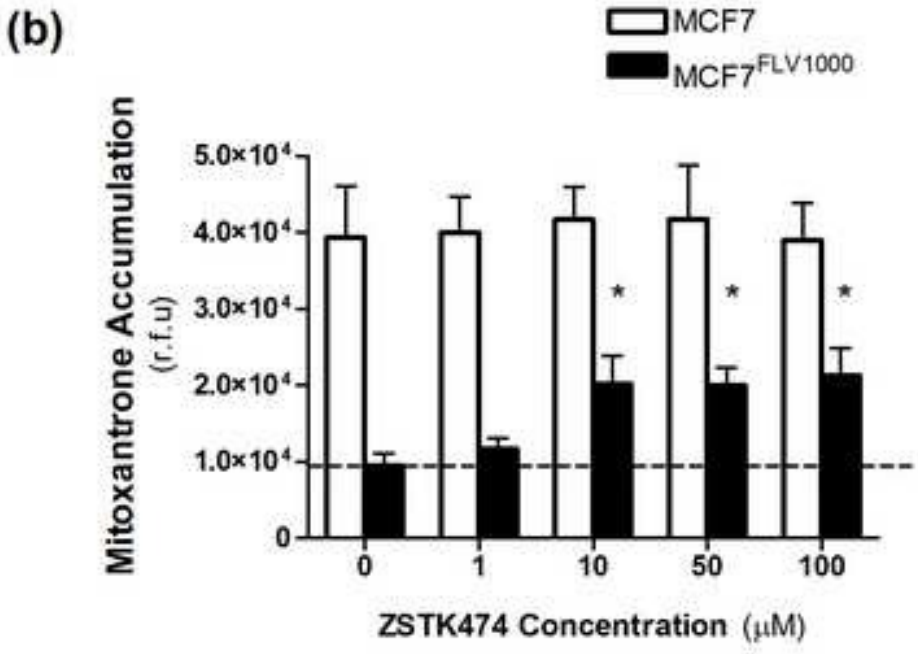

FIGURE 6

Figure 7

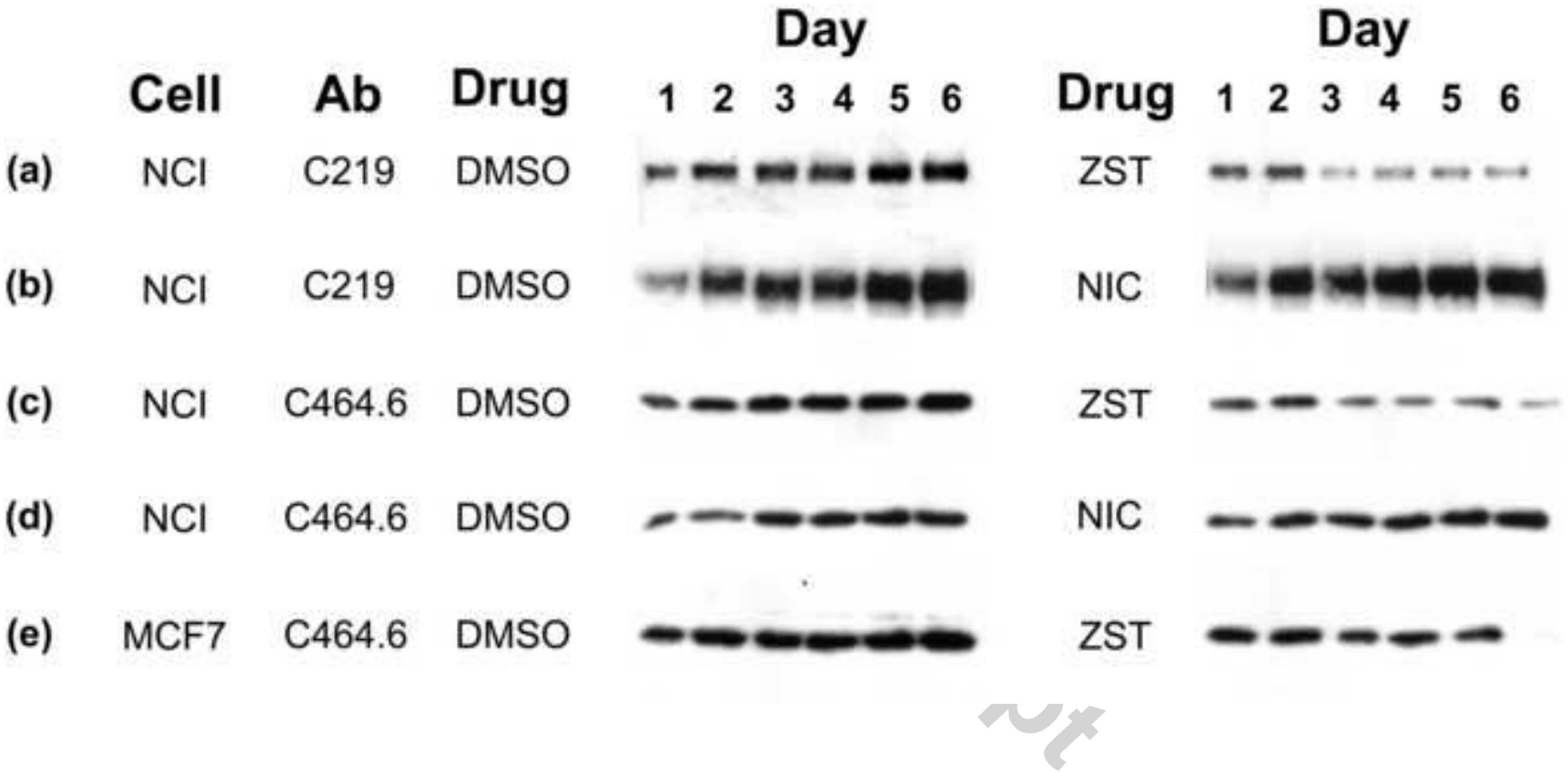

ACCEPTED MANUSCRIPT

ACCEPTED MANUSCRIPT

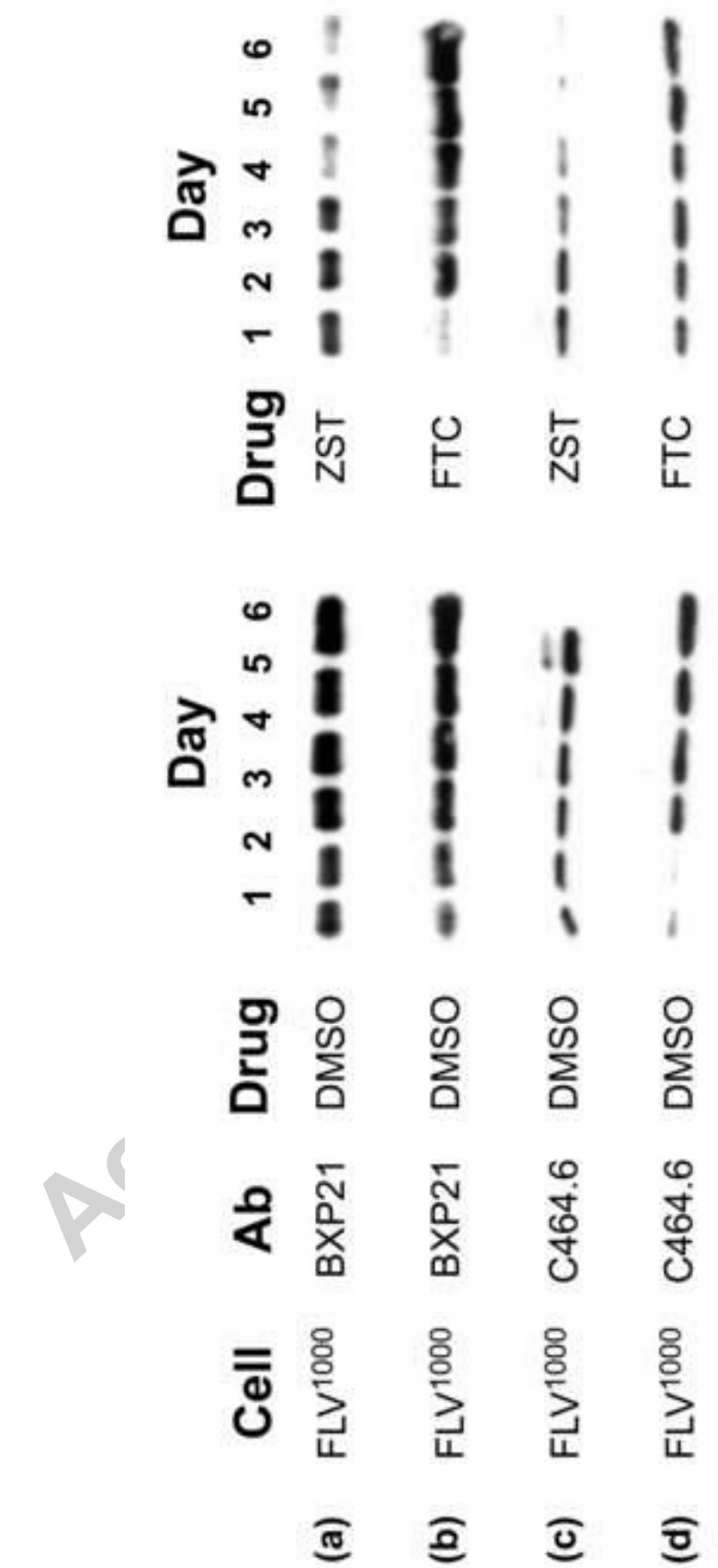

Figure 8

Figure 9

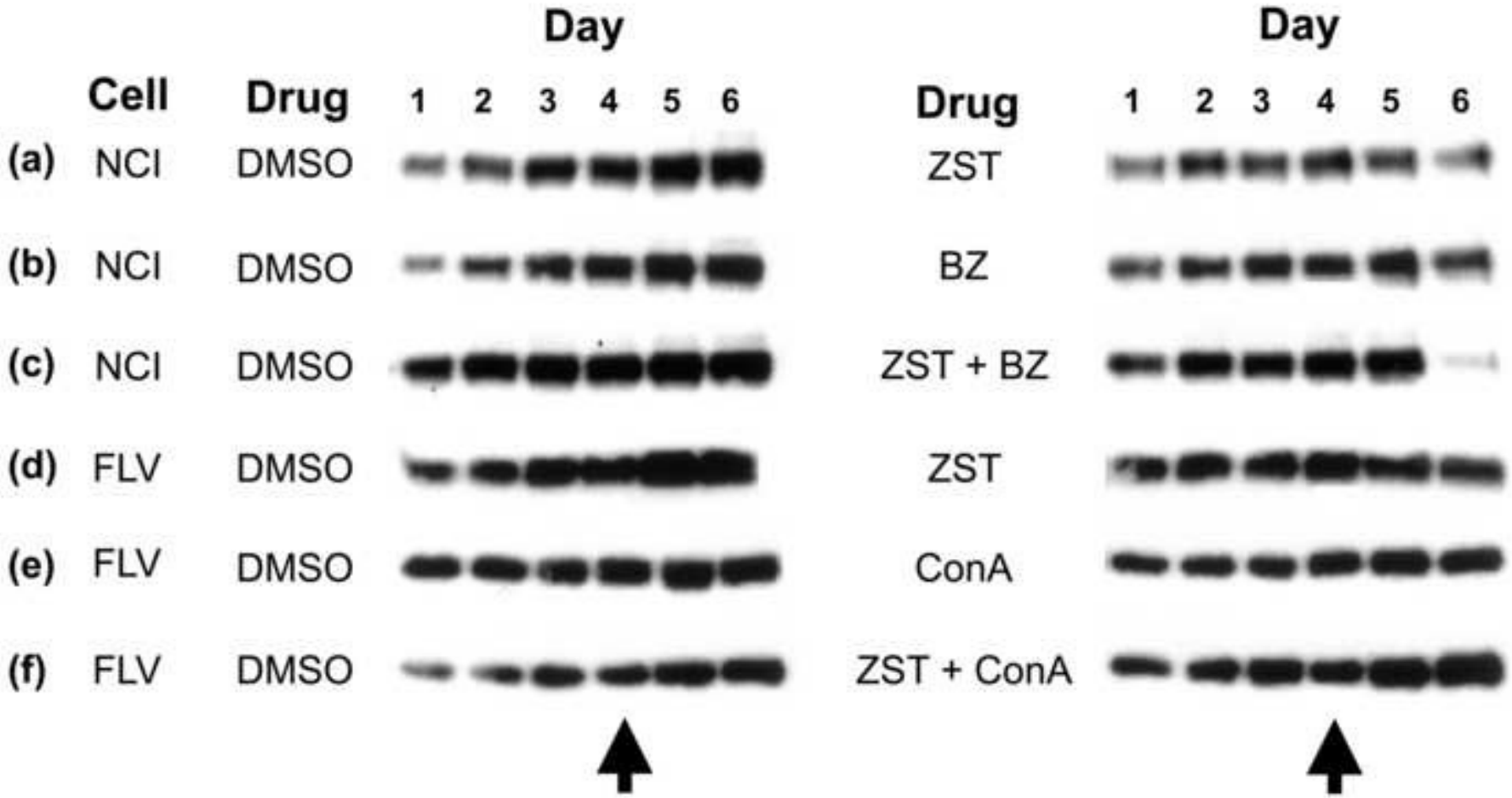

ACCEPTED MANUSCRIPT

Figure 10

ACCEPTED MANUSCRIPT

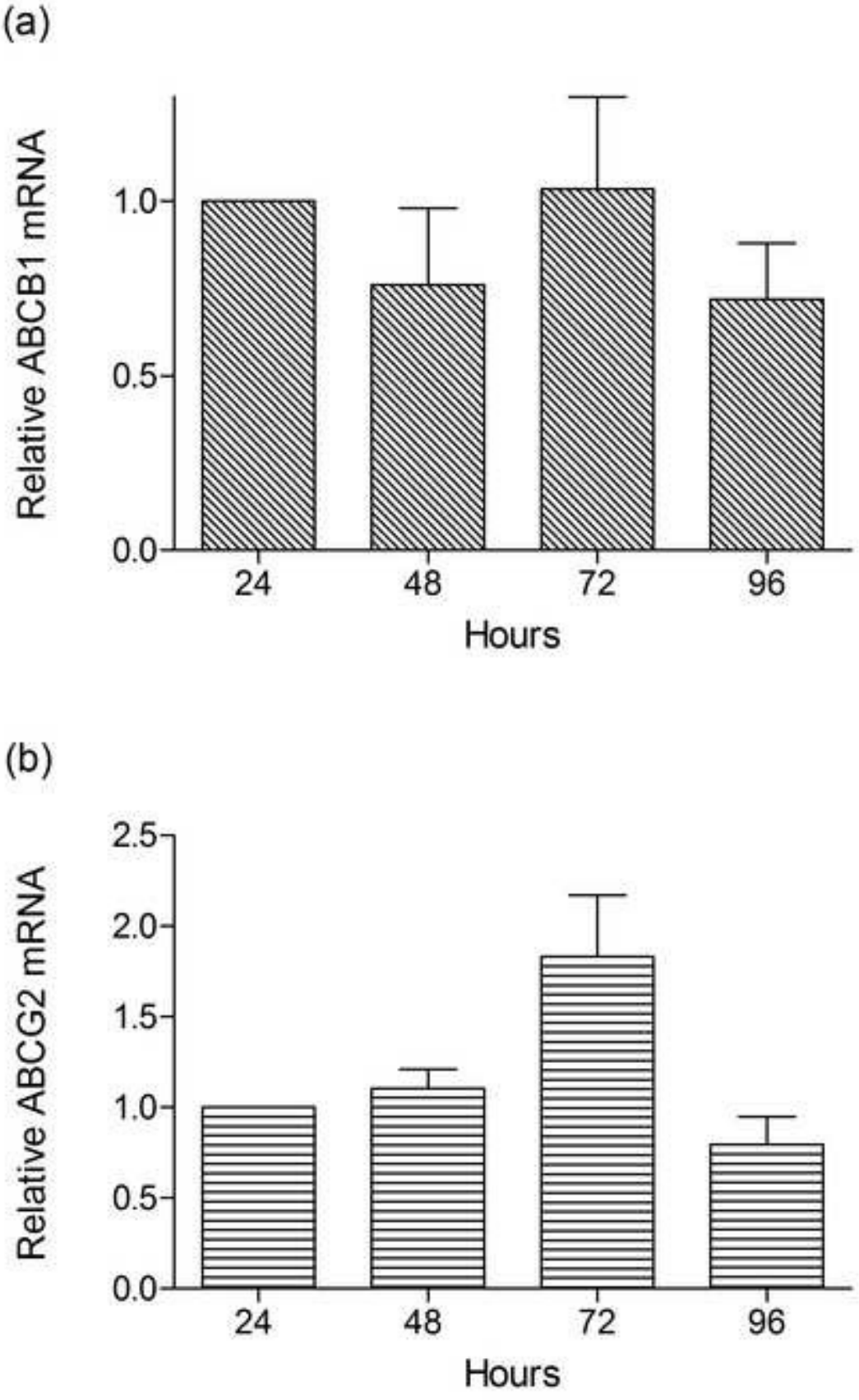

FIGURE 10

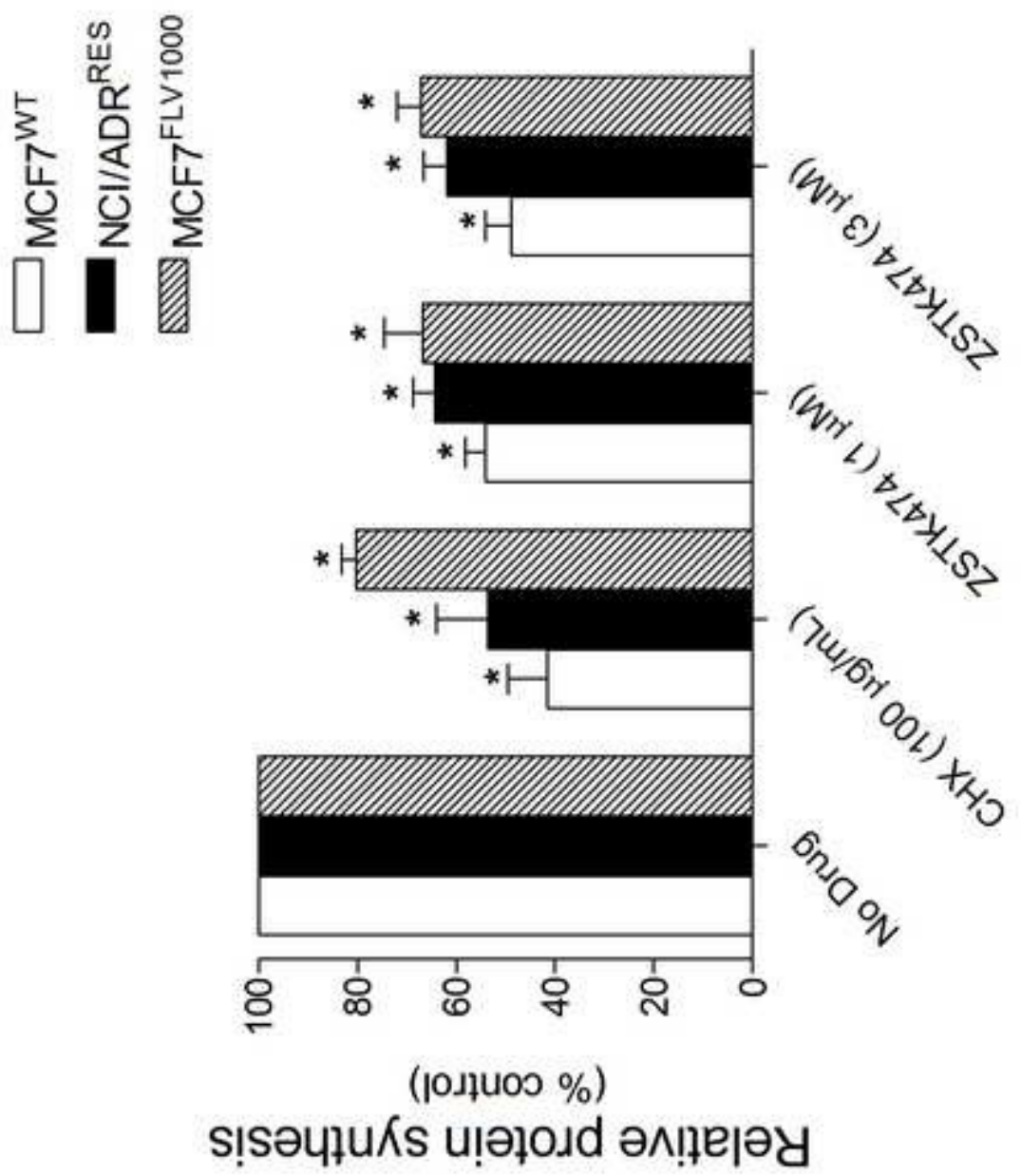

FIGURE 11

Figure 11

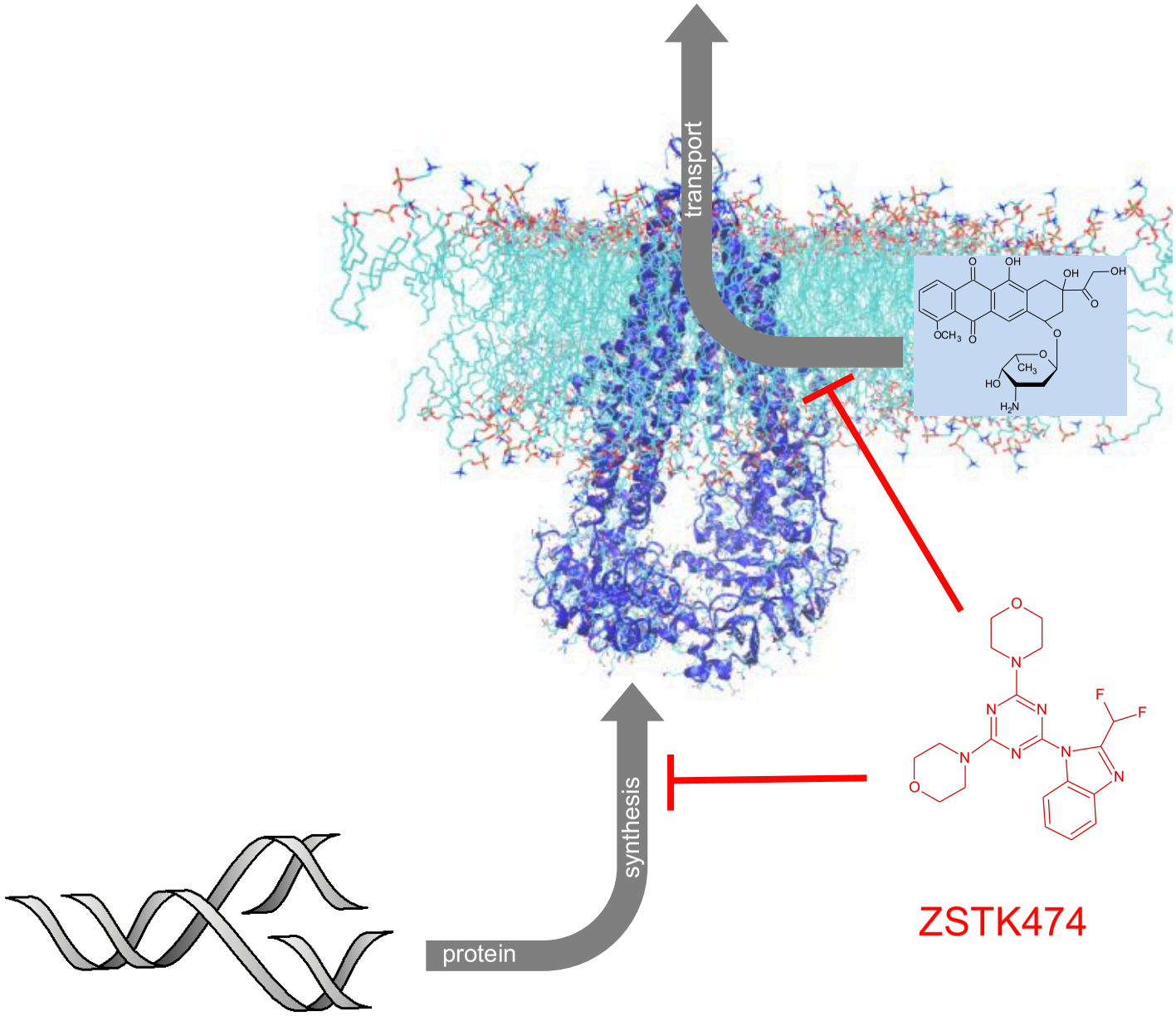

Graphic Abstract - Muthiah & Callaghan

ACCEPTED MANUSCRIPT